

periportal or perisinusoidal fibrosis; stage 2, periportal plus perisinusoidal fibrosis; and stage 3, bridging fibrosis.²⁴

Quantitative RT-PCR

Total RNA was extracted from the liver and epididymal white adipose tissue using Sepasol reagent (Nacalai Tesque, Inc., Kyoto, Japan). Quantitative RT-PCR was performed using the ABI Prism 7000 Sequence Detection System with PCR Master Mix Reagent (Applied Biosystems, Inc., Foster City, CA) as described previously.²³ Primers used are given in Table 1. mRNA levels were normalized to those of 36B4 mRNA.

Measurement of Serum Hydroperoxides

The total amount of organic hydroperoxides in the serum was measured at spectrophotometry using the derivatives of reactive oxygen metabolites test (FREE Carpe Diem; Diacron International SAS, Grosseto, Italy). Hydroperoxides are intermediate oxidative products of lipids, peptides, and amino acids, and their concentrations represent an index of oxidative injury. This method is described in detail elsewhere.²⁵ In brief, 20- μ L serum samples were added to 1 mL assay mixture, gently mixed, and incubated for 3 minutes at 37°C. The absorbance increase at 505 nm was monitored for 2 minutes. The concentrations were expressed in conventional units [Carratelli units (U.CARR)], where 1 U.CARR corresponds to 0.8 mg/L H₂O₂.

TG Secretion Rate

The TG secretion rate was measured as previously described.²⁶ In brief, 500 mg/kg body weight tyloxapol (Triton WR-1339; Sigma-Aldrich Corp., St. Louis, MO) was injected via the tail vein into mice that had been fasted for 5 hours. Serum TG concentrations were measured at 60 minutes after injection. The TG secretion rate was calculated from the increment in TG concentration per minute multiplied by the serum volume of mice (estimated as 3.5% of body weight in grams) and expressed in milligrams per minute per 100 g body weight.

Statistical Analysis

Data are given as mean \pm SE. *P* < 0.05 was considered statistically significant. Statistical analysis was performed using analysis of variance followed by Scheffé's test.

Results

Metabolic Phenotypes of MC4R-KO Mice

Throughout the experimental period, MC4R-KO mice demonstrated accelerated body weight gain relative to WT mice fed either the standard diet or the HFD (Figure 1A). Both the WT mice fed the HFD and the MC4R-KO

Table 1. Primers Used in the Present Study

Genes	Primers
<i>ACC1</i>	
Forward	5'-TGAGATTGGCATGGTAGCCTG-3'
Reverse	5'-CTCGCCATCTGGATATTCAG-3'
<i>Catalase</i>	
Forward	5'-GGAGGCAGAACTTTCCATT-3'
Reverse	5'-GGCCAAACCTTGGTCAGATC-3'
<i>COL1A1</i>	
Forward	5'-CCTCAGGGTATTGCTGGACAAC-3'
Reverse	5'-ACCACTTGATCCAGAAGGACCTT-3'
<i>CPT1A</i>	
Forward	5'-CCTGCATTCCTCCCATTTG-3'
Reverse	5'-TGCCCATGTCTTGTAAATGTG-3'
<i>F4/80</i>	
Forward	5'-CTTTGGCTATGGGCTTCCAGT-3'
Reverse	5'-GCAAGGAGGACAGAGTTTATCGTG-3'
<i>FAS</i>	
Forward	5'-CCTGGATAGCATTCGGAACCT-3'
Reverse	5'-AGCACATCTCGAAGGCTACACA-3'
<i>gp91^{phox}</i>	
Forward	5'-CCAGTGCGTGTGTGCTCGA-3'
Reverse	5'-AGTGAGGTTCCGTCCAGTTGTCT-3'
<i>MMP-2</i>	
Forward	5'-CCCCATGAAGCCTTGTTTACC-3'
Reverse	5'-TTGTAGGAGGTGCCCTGGAA-3'
<i>MTP</i>	
Forward	5'-ACAGGTCTCGAGCGTGTCT-3'
Reverse	5'-CAGTGTCCGCCAGAGAAG-3'
<i>p22^{phox}</i>	
Forward	5'-CATGGAGCGATGTGGACAGA-3'
Reverse	5'-CCCGAAAAGCTTCAACCACAG-3'
<i>p40^{phox}</i>	
Forward	5'-CAGCCAACATCGCTGACATC-3'
Reverse	5'-CAAAGTGGCTGTTGAAGCCC-3'
<i>p47^{phox}</i>	
Forward	5'-ACTTCTACTGAATACTTCAACG-3'
Reverse	5'-TCATCAGGCCGCACTTT-3'
<i>p67^{phox}</i>	
Forward	5'-AAGCAAAAAGAGCCCAAGGAA-3'
Reverse	5'-CATGTAAGGCATAGGCACGCT-3'
<i>PPARα</i>	
Forward	5'-AGGAAGCGTTCTGTGACAT-3'
Reverse	5'-AATCCCCCTCTGCAACTTCT-3'
<i>SOD1</i>	
Forward	5'-GCAGGACCTCATTTTAATCCTCACT-3'
Reverse	5'-AGGTCTCCAACATGCCTCTCTTTC-3'
<i>SREBP1c</i>	
Forward	5'-GGCACTAAGTGCCCTCAACCT-3'
Reverse	5'-GCCACATAGATCTCTGCCAGTGT-3'
<i>TGFβ1</i>	
Forward	5'-CCTGAGTGGCTGTCTTTTGACG-3'
Reverse	5'-AGTGAGCGCTGAATCGAAAGC-3'
<i>TIMP1</i>	
Forward	5'-CATCACGGGCCCTA-3'
Reverse	5'-AAGCTGCAGGCACTGATGTG-3'
<i>TNFα</i>	
Forward	5'-ACCCTCACACTCAGATCATCTTC-3'
Reverse	5'-TGGTGGTTTGCTACGACGT-3'
<i>36B4</i>	
Forward	5'-GGCCCTGCACCTCTCGCTTTC-3'
Reverse	5'-TGCCAGGACGCGCTTGT-3'

mice fed the standard diet exhibited increased adiposity relative to the WT mice fed the standard diet (Figure 1B). Although increased adiposity was observed in MC4R-KO mice at 8 weeks of HFD feeding, there was no further increase or decrease in adipose tissue weight thereafter (Figure 1B). In contrast, MC4R-KO mice exhibited a time-dependent increase in liver

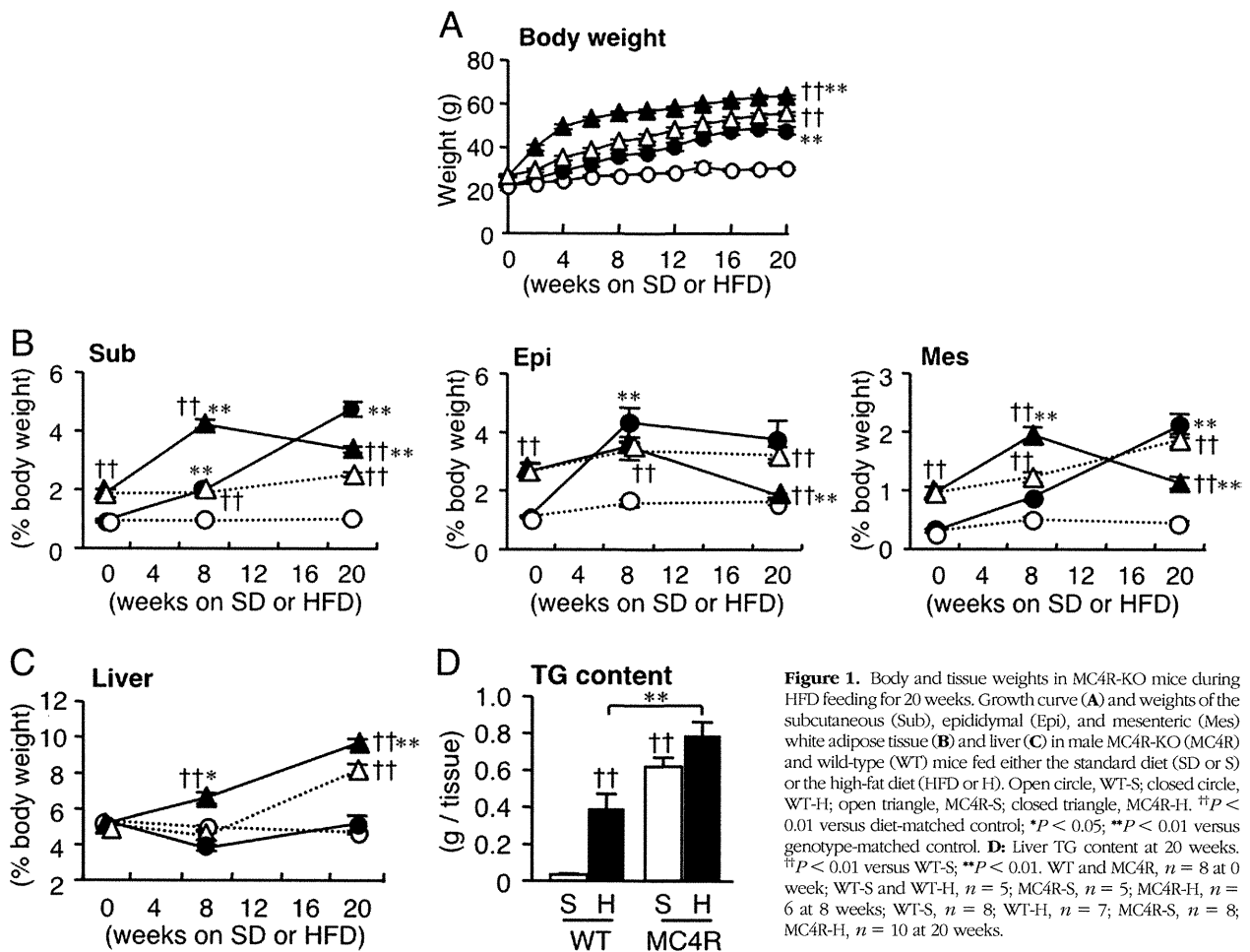


Figure 1. Body and tissue weights in MC4R-KO mice during HFD feeding for 20 weeks. Growth curve (A) and weights of the subcutaneous (Sub), epididymal (Epi), and mesenteric (Mes) white adipose tissue (B) and liver (C) in male MC4R-KO (MC4R) and wild-type (WT) mice fed either the standard diet (SD or S) or the high-fat diet (HFD or H). Open circle, WT-S; closed circle, WT-H; open triangle, MC4R-S; closed triangle, MC4R-H. ††*P* < 0.01 versus diet-matched control; **P* < 0.05; ***P* < 0.01 versus genotype-matched control. D: Liver TG content at 20 weeks. ††*P* < 0.01 versus WT-S; ***P* < 0.01. WT and MC4R, *n* = 8 at 0 week; WT-S and WT-H, *n* = 5; MC4R-S, *n* = 5; MC4R-H, *n* = 6 at 8 weeks; WT-S, *n* = 8; WT-H, *n* = 7; MC4R-S, *n* = 8; MC4R-H, *n* = 10 at 20 weeks.

weight and hepatic TG content relative to WT mice fed either diet (Figure 1, C and D; and data not shown). Both genotypes fed the HFD exhibited insulin resistance, and MC4R-KO mice fed the HFD exhibited a significant increase in serum FFA concentrations relative to WT mice (Table 2). Dysregulation of adipocytokines was also marked in MC4R-KO mice fed the HFD relative to WT mice (Table 2, and Supplemental Table

S2 at <http://ajp.amjpathol.org>). Serum alanine aminotransferase concentrations were significantly increased in MC4R-KO mice fed the HFD relative to any other groups (Table 2). In essence, these observations are consistent with previous reports that described the metabolic phenotypes in the liver in MC4R-KO mice, which were generated using different strategies.^{18,19} Collectively, our data indicate that MC4R-KO mice fed

Table 2. Serologic Parameters of MC4R-KO and WT Mice Fed the HFD for 20 Weeks

Variable	WT mice		MC4R-KO mice	
	SD	HFD	SD	HFD
Blood glucose (<i>ad lib</i> , mg/dL)	117.3 ± 5.8	133.0 ± 8.3	167.4 ± 10.3*	170.1 ± 12.4
HOMA-IR	0.8 ± 0.3	15.5 ± 3.7*	17.0 ± 4.0†	21.8 ± 3.7
TG (mg/dL)	84.6 ± 9.8	46.3 ± 1.2*	135.8 ± 18.4*	92.7 ± 8.1
FFA (mEq/L)	0.27 ± 0.02	0.26 ± 0.01	0.34 ± 0.02	0.51 ± 0.06 ^{‡§}
TC (mg/dL)	51.6 ± 2.8	189.7 ± 6.4†	143.0 ± 9.5*	294.5 ± 9.2 ^{†¶}
Adiponectin (μg/mL)	15.4 ± 1.7	19.8 ± 1.7	13.5 ± 1.0	8.2 ± 0.9 ^{‡§}
Leptin (ng/mL)	1.7 ± 0.3	97.2 ± 8.3†	57.7 ± 6.0†	112.6 ± 9.2 [¶]
IL-6 (pg/mL)	0.84 ± 0.64	2.21 ± 1.68	3.25 ± 0.75	6.80 ± 0.71 [¶]
ALT (IU/L)	36.9 ± 1.1	129.9 ± 19.6	191.9 ± 29.2*	623.9 ± 50.8 ^{†¶}

n = 7–10. Data are expressed as mean ± SE.

**P* < 0.05, †*P* < 0.01 versus WT-SD; ‡*P* < 0.01 versus WT-HFD; §*P* < 0.05; ¶*P* < 0.01 versus MC4R-SD.

ALT, alanine aminotransferase; FFA, free fatty acid; HFD, high-fat diet; HOMA-IR, homeostasis model assessment–insulin resistance; IL-6, interleukin-6; SD, standard diet; TC, total cholesterol; TG, triglyceride; WT, wild-type.

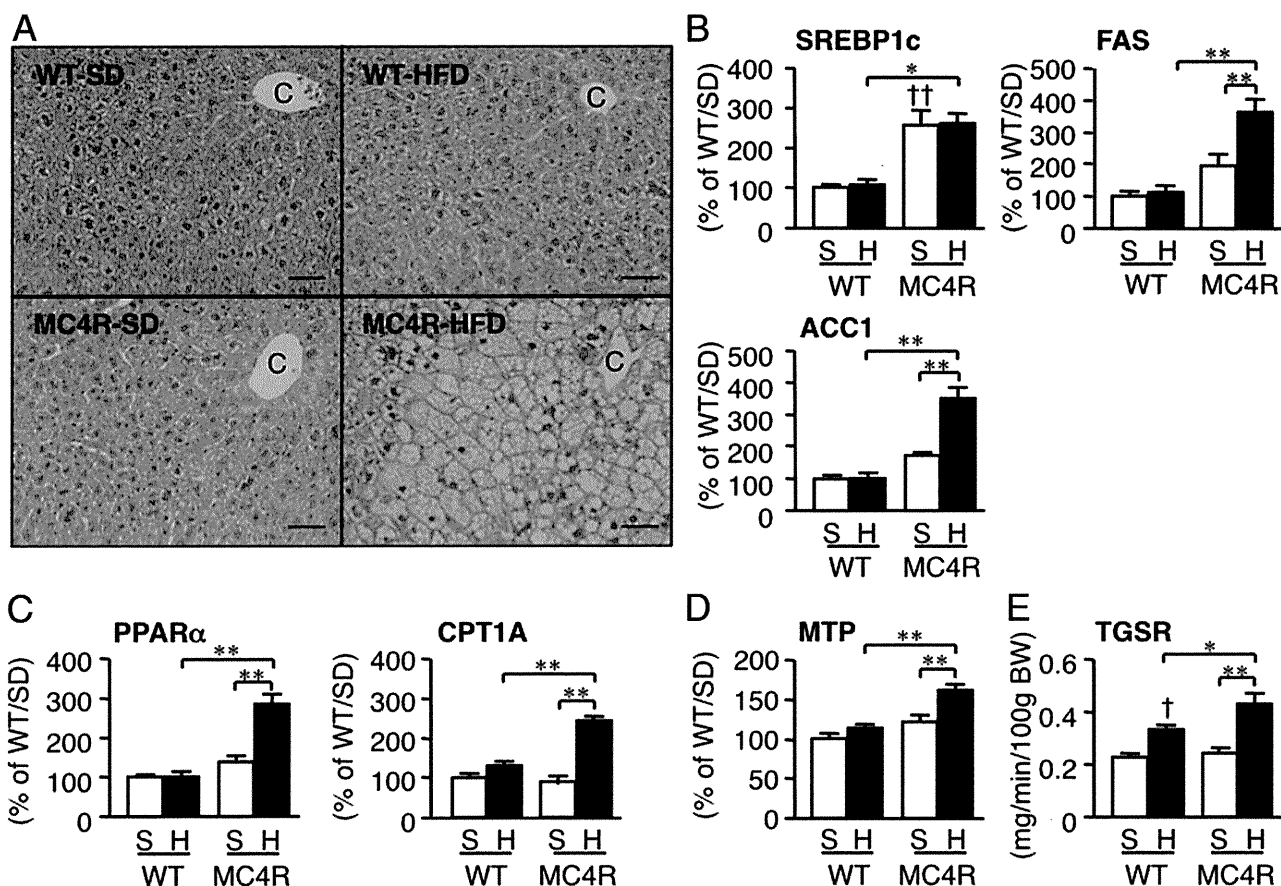


Figure 2. Hepatic histologic features and mRNA expression of genes related to lipid metabolism in MC4R-KO and WT mice fed the HFD for 8 weeks. **A:** H&E staining of the liver. C, central vein. Original magnification, $\times 200$. Scale bar = $50 \mu\text{m}$. Hepatic mRNA expression of genes for *de novo* lipogenesis (sterol regulatory element binding protein 1c, fatty acid synthase, and acetyl-CoA carboxylase 1) (**B**), oxidative metabolism (peroxisome proliferator-activated receptor- α and carnitine palmitoyltransferase 1A) (**C**), and TG secretion (microsomal TG transport protein) (**D**). **E:** Triglyceride secretion rate from the liver at 2 weeks of HFD feeding. * $P < 0.05$; ** $P < 0.01$; † $P < 0.05$; †† $P < 0.01$ versus WT-S. WT-S and WT-H, $n = 5$; MC4R-S, $n = 5$; MC4R-H, $n = 6$.

the HFD exhibit metabolic characteristics similar to those in obese humans.

Lipid Metabolism and Oxidative Stress in Liver from MC4R-KO Mice

Next examined was lipid metabolism and oxidative stress in liver from MC4R-KO mice fed the HFD. Although histologic examinations revealed minimal lipid accumulation in liver from WT mice fed the HFD for 8 weeks, liver from MC4R-KO mice exhibited massive microvesicular steatosis in the centrilobular and portal areas (Figure 2A). Expression of mRNAs for *de novo* lipogenesis (fatty acid synthase and acetyl-CoA carboxylase 1) was markedly increased in liver from MC4R-KO mice relative to WT mice at 8 weeks (Figure 2B), as previously reported.^{18,19} In addition, expression of mRNAs for fatty acid oxidation (peroxisome proliferator-activated receptor- α and carnitine palmitoyltransferase 1A), and TG secretion (microsomal triglyceride transport protein) and TG secretion rate were increased in liver from MC4R-KO mice (Figure 2, C–E). These observations are consistent with lipid metabolism in human NASH.²⁷ In contrast to the changes in hepatic expression of lipogenic genes in MC4R-KO mice (Figure 2B), WT mice exhibited up-regulation of lipogenic

genes only after 20 weeks of HFD feeding (data not shown), which suggests that hepatic steatosis develops much faster in MC4R-KO mice than in WT mice. There was a marked increase in mRNA expression of the NADPH oxidase components (p40^{phox}, p47^{phox}, p67^{phox}, gp91^{phox}, and p22^{phox}), and a slight increase in mRNA expression of antioxidant enzymes (superoxide dismutase 1 and catalase) in the HFD-fed MC4R-KO mice relative to any other groups (see Supplemental Figure S1, A and B, at <http://ajp.amjpathol.org>). Serum concentrations of derivatives of reactive oxidative metabolite were significantly increased in MC4R-KO mice fed the HFD ($P < 0.01$; see also Supplemental Figure S1C at <http://ajp.amjpathol.org>).

Lipid Accumulation and Fibrosis in Liver from MC4R-KO Mice

After HFD feeding for 20 weeks, microvesicular steatosis was observed uniformly, and moderate inflammatory cell infiltration in liver from WT mice (Figure 3A), whereas liver fibrosis was rarely observed at this time point (Figure 3, B–D). In contrast, liver from MC4R-KO mice fed the HFD exhibited microvesicular and macrovesicular steatosis, ballooning degeneration, and

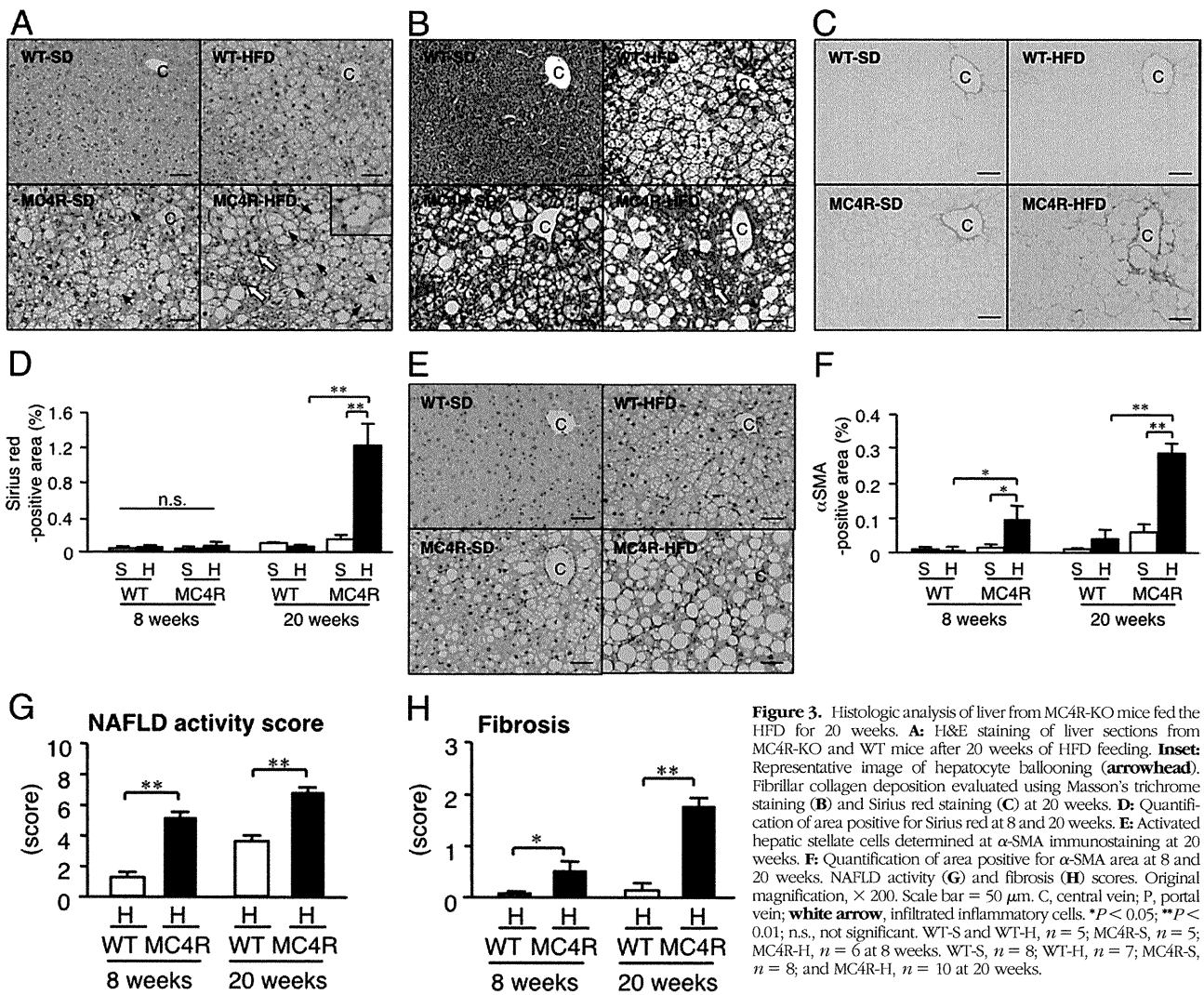


Figure 3. Histologic analysis of liver from MC4R-KO mice fed the HFD for 20 weeks. **A:** H&E staining of liver sections from MC4R-KO and WT mice after 20 weeks of HFD feeding. **Inset:** Representative image of hepatocyte ballooning (arrowhead). Fibrillar collagen deposition evaluated using Masson's trichrome staining (**B**) and Sirius red staining (**C**) at 20 weeks. **D:** Quantification of area positive for Sirius red at 8 and 20 weeks. **E:** Activated hepatic stellate cells determined at α -SMA immunostaining at 20 weeks. **F:** Quantification of area positive for α -SMA area at 8 and 20 weeks. **G:** NAFLD activity (**G**) and fibrosis (**H**) scores. Original magnification, $\times 200$. Scale bar = 50 μ m. C, central vein; P, portal vein; **white arrow**, infiltrated inflammatory cells. * $P < 0.05$; ** $P < 0.01$; n.s., not significant. WT-S and WT-H, $n = 5$; MC4R-S, $n = 5$; MC4R-H, $n = 6$ at 8 weeks. WT-S, $n = 8$; WT-H, $n = 7$; MC4R-S, $n = 8$; and MC4R-H, $n = 10$ at 20 weeks.

massive infiltration of inflammatory cells (Figure 3A). Masson's trichrome and Sirius red staining revealed marked pericellular fibrosis in liver from MC4R-KO mice fed the HFD (Figure 3, B–D). In addition, the area positive for α -SMA was markedly increased in MC4R-KO mice relative to WT mice fed the HFD for 8 and 20 weeks ($P < 0.05$ and $P < 0.01$, respectively; Figure 3, E and F). Histologic analysis demonstrated a significant increase in the NAFLD activity and fibrosis scores in MC4R-KO mice at 8 and 20 weeks of HFD feeding (Figure 3, G and H). Expression of mRNAs for fibrogenic genes (transforming growth factor- β 1; collagen, type 1, α 1; metalloproteinase-2; and tissue inhibitor of metalloproteinase 1), and inflammatory genes (macrophage marker F4/80 and tumor necrosis factor- α) was increased in liver from MC4R-KO mice relative to WT mice after 20 weeks of HFD feeding (Figure 4). Together, these observations suggest that MC4R-KO mice fed the HFD develop liver fibrosis accompanied by histologic pathognomonic features of human NASH: inflammatory cell infiltration, hepatocyte ballooning, and pericellular fibro-

Development of HCC in MC4R-KO Mice

After feeding the HFD for 1 year, mild fibrosis was observed in WT mice, which was much more accelerated in MC4R-KO mice (see Supplemental Figure S2 at <http://ajp.amjpathol.org>). Moreover, multiple liver tumors were observed in all of the MC4R-KO mice examined ($n = 5$) (Figure 5A). Microscopic analysis revealed that the tumors form discrete nodules surrounded by non-tumor liver tissue (Figure 5B). Normal liver architecture was lost, and irregular and thick trabeculae were observed in the tumors (Figure 5C). The tumor cells exhibited severe dysplasia, with an increased nuclear-cytoplasmic ratio, enlarged and hyperchromatic nuclei, and fat deposition in the cytoplasm (Figure 5C). Immunohistochemical analysis revealed that the tumors express α -fetoprotein, a widely recognized marker of HCC (Figure 5D). In contrast, at 20 weeks and even at 1 year, there was no appreciable collagen deposition and tumor development in liver from MC4R-KO mice fed the standard diet (Figures 3; see also Supplemental Figure S2 at <http://ajp.amjpathol.org>). To elucidate the involvement of the inher-

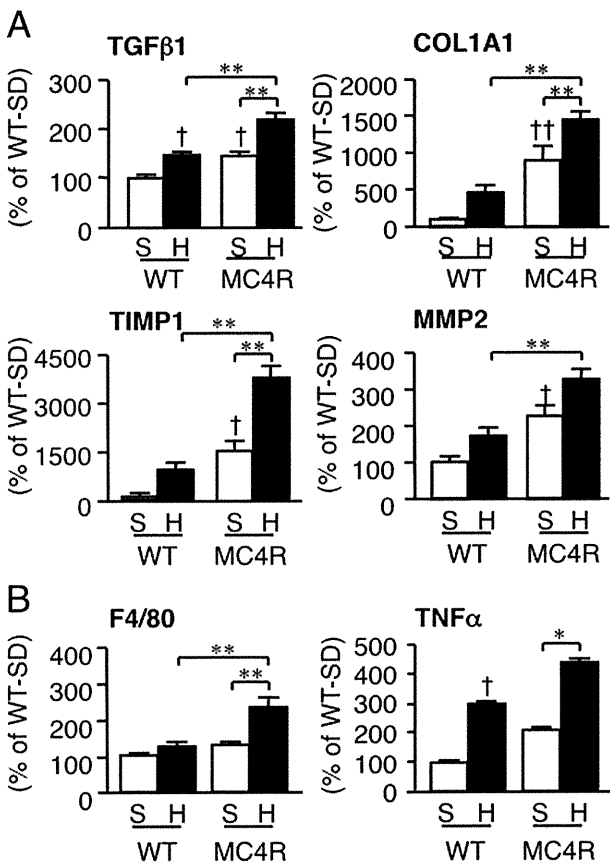


Figure 4. Hepatic mRNA expression in MC4R-KO mice fed the HFD for 20 weeks. Hepatic mRNA expression levels were measured using quantitative PCR after 20 weeks of HFD feeding. mRNA expression of fibrogenic factors (transforming growth factor- β 1; collagen, type 1, α 1; tissue inhibitor of metalloproteinase 1; and metalloproteinase 2) (A) and inflammatory markers (F4/80 and tumor necrosis factor- α) (B). * $P < 0.05$; ** $P < 0.01$; † $P < 0.05$; †† $P < 0.01$ versus WT-S. WT-S, $n = 8$; WT-H, $n = 7$; MC4R-S, $n = 8$; and MC4R-H, $n = 10$.

ent dysregulation of inflammation and fibrogenesis in MC4R-KO mice, we examined the liver and adipose tissue phenotypes in 8 week-old MC4R-KO and WT mice. There was no significant difference in mRNA expression of pro-fibrotic and inflammatory genes between the genotypes at this time point (see Supplemental Figure S3 at <http://ajp.amjpathol.org>). These observations suggest that in addition to liver fibrosis, MC4R-KO mice fed the HFD develop multiple liver tumors with histologic characteristics of well-differentiated HCC.

Inflammatory and Fibrotic Changes in Adipose Tissue from MC4R-KO Mice

Recent evidence has suggested that obese adipose tissue exhibits chronic inflammatory changes characterized by macrophage infiltration and fibrosis, which may contribute to ectopic lipid accumulation and systemic insulin resistance.^{28,29} In the present study, macrophage infiltration and pro-inflammatory cytokine expression were markedly increased in the epididymal white adipose tissue from MC4R-KO mice relative to WT mice after 8 weeks of HFD feeding, although the epididymal white

adipose tissue weight was almost comparable between the genotypes (Figure 1B and Figure 6, A and B). Moreover, a marked increase was observed in collagen deposition and in transforming growth factor β 1 and in collagen, type 1, α 1 mRNA expression in the epididymal white adipose tissue from MC4R-KO mice relative to WT mice (Figure 6, C and D). These observations suggest that adipose tissue inflammation is markedly enhanced in MC4R-KO mice relative to WT mice during HFD feeding, along with dysregulation of adipocytokine production in MC4R-KO mice (see Supplemental Table S2 at <http://ajp.amjpathol.org>).

Discussion

According to the two-hit hypothesis, the pathogenesis of NASH may involve at least two processes: excessive accumulation of lipids in the liver and enhanced liver fibrosis. To understand the molecular mechanism underlying the development of NASH, many animal models of hepatic steatosis and liver fibrosis have been described. Herein we demonstrate that MC4R-KO mice fed an HFD for a relatively short time (20 weeks) exhibit a liver condition similar to human NASH, in addition to obesity and insulin resistance. As a model of hyperphagic obesity, *ob/ob* mice exhibit severe hepatic steatosis, although

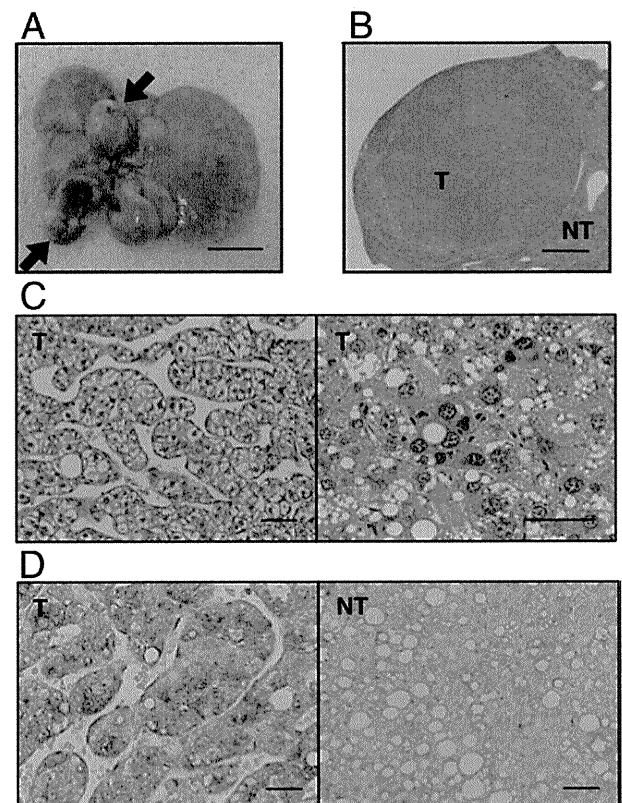


Figure 5. Development of hepatocellular carcinoma in liver from MC4R-KO mice after 1 year of HFD feeding. All MC4R-KO mice ($n = 5$) developed multiple liver tumors (arrows). A: Representative macroscopic image of liver from MC4R-KO mice. H&E staining (B and C) and α -fetoprotein immunostaining (D) of the tumor. NT, non-tumor liver; T, tumors. Scale bars: 1 cm (A); 1 mm (B); 50 μ m (C and D).

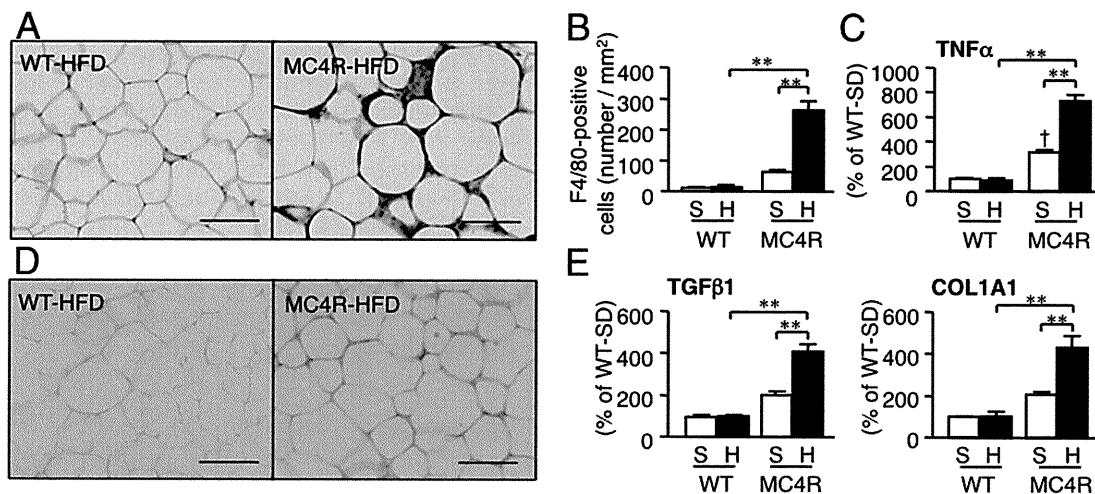


Figure 6. Inflammatory changes in epididymal white adipose tissue from MC4R-KO mice fed the HFD. Representative F4/80 immunostaining (A) and quantification of F4/80-positive cells (B) of the epididymal white adipose tissue from MC4R-KO and WT mice fed the HFD for 8 weeks. Original magnification, $\times 200$. Scale bar = 100 μ m. C: Tumor necrosis factor- α mRNA expression in the epididymal white adipose tissue. Sirius red staining of epididymal white adipose tissue (D) and mRNA expression of fibrogenic genes (transforming growth factor- β 1; and collagen, type 1, α 1) (E). ** $P < 0.01$; † $P < 0.05$ versus WT-S. WT-S and WT-H, $n = 5$; and MC4R-S, $n = 5$, MC4R-H, $n = 6$.

they are resistant to liver fibrosis.³ Moreover, animals with diet-induced obesity exhibit hepatic steatosis and develop mild liver fibrosis only after long-term (usually longer than 1 year) HFD feeding,^{30,31} as was observed in the present study. In contrast, chemically induced liver fibrosis is not accompanied by obesity, insulin resistance, and hepatic steatosis.³ Dietary deficiency of methionine and choline also contribute to development of steatosis and mild fibrosis, without obesity and insulin resistance.³ In this regard, Larter et al³² recently reported that *foz/foz* mice, carrying truncating mutation in *Alms1*, demonstrated both obesity and NASH-like liver histologic features during long-term feeding of an HFD. This study has established MC4R-KO mice fed the HFD for a relatively short time as a novel rodent model of NASH with obesity, insulin resistance, and excessive accumulation of lipids and enhanced fibrosis in the liver.

NASH is a severe form of NAFLD, and can progress to cirrhosis and HCC. However, there have been no appropriate animal models in which NASH progressed to HCC during the course of obesity. Indeed, there are a few genetic models of liver fibrosis and HCC: mice with liver-specific disruption of phosphatase and tensin homolog deleted from chromosome 10 and those lacking methionine adenosyltransferase 1A, although they do not exhibit obesity and insulin resistance.^{33,34} In the present study, we have demonstrated that MC4R-KO mice, when fed the HFD over the long term, develop multiple liver tumors with histologic characteristics of well-differentiated HCC. In MC4R-KO mice fed the HFD, enhanced pro-inflammatory cytokine production and fibrotic changes preceded development of multiple liver tumors, which is consistent with a recent report by Park et al³⁵ that increased production of tumor necrosis factor- α and IL-6 in obesity is involved in promotion of carcinogen-induced hepatic tumorigenesis. Collectively, MC4R-KO mice would provide a novel mouse model of NASH with which to investigate the sequence of events that make up diet-induced he-

patic steatosis, liver fibrosis, and HCC or how overnutrition leads to hepatic steatosis and liver fibrosis and eventually to HCC.

During the course of obesity, there might be complex interactions between the adipose tissue and the liver (the adipohepatic axis) in the pathogenesis of NASH.^{6,7} In the present study, enhanced adipose tissue inflammation, ie, increased macrophage infiltration and fibrotic changes, was observed in MC4R-KO mice relative to WT mice during the HFD feeding. We previously have demonstrated that cross-talk between adipocytes and macrophages in obese adipose tissue results in marked up-regulation of pro-inflammatory adipocytokines such as tumor necrosis factor- α and significant down-regulation of anti-inflammatory adiponectin.³⁶ Of note, saturated fatty acids, which are released in large quantities from hypertrophied adipocytes via macrophage-induced lipolysis, may act as an endogenous ligand for the Toll-like receptor 4 complex.³⁷ Moreover, FFAs, when overproduced in the visceral fat depots through the cross-talk between adipocytes and macrophages, may enter the liver via the portal vein. Indeed, MC4R-KO mice demonstrated increased serum concentrations of FFA relative to WT mice during the HFD feeding. It is, therefore, likely that enhanced adipose tissue inflammation in MC4R-KO mice causes dysregulation of adipocytokine production and FFA release, thereby contributing to the NASH-like hepatic phenotype. Also observed was a marked increase in collagen deposition in white adipose tissue from MC4R-KO mice. Khan et al³⁸ recently reported that in collagen VI-deficient mice extracellular matrix components, when increased in obese adipose tissue, inhibited adipose tissue expansion. This is consistent with a recent clinical study that demonstrated that adipose tissue fibrosis is negatively correlated with adipocyte diameter in obese humans.³⁹ Moreover, McQuaid et al⁴⁰ reported that the lipid storage function in adipose tissue is negatively associated with ectopic lipid accumulation in obese

humans. It is, therefore, conceivable that both adipose tissue macrophage infiltration and fibrotic changes increase the release of FFAs, thereby contributing to excessive fat accumulation in the liver in MC4R-KO mice. Together, these observations suggest that enhanced adipose tissue inflammation has a role in development of NASH as both the first and second hits in MC4R-KO mice. These data suggest that MC4R-KO mice are useful for investigation of the role of the adipohepatic axis in the development of NASH.

Because MC4R mRNA expression is restricted to the hypothalamus and other brain regions⁴¹ and is undetectable in liver from WT mice fed the HFD (Itoh et al, unpublished data, 2010), it is likely that the hepatic phenotype in MC4R-KO mice results from loss of function of MC4R in the brain. In the present study, MC4R-KO mice demonstrated increased expression of mRNAs for *de novo* lipogenesis, fatty acid oxidation, and TG secretion relative to WT mice fed the HFD. This is consistent with a recent report by Nogueiras et al⁴² that short-term pharmacologic blockade of the central melanocortin system in WT mice results in increased expression of *de novo* lipogenic genes and microsomal TG transport protein in the liver. Evidence has accumulated suggesting that the brain and liver interact via neuronal pathways, central insulin signaling regulates glucose metabolism in the liver, and peroxisome proliferator-activated receptor- γ activation in the liver modulates energy expenditure and systemic insulin sensitivity via the sympathetic nervous system.^{43,44} In this regard, we previously reported that the central melanocortin system is involved in renal macrophage infiltration in a mouse model of renal fibrosis.²¹ This discussion also supports the concept that MC4R signaling in the brain is involved in excessive accumulation of lipids and fibrosis in the liver in MC4R-KO mice.

Because MC4R-KO mice exhibited hyperleptinemia, leptin signaling may have a role in the pathogenesis of the hepatic liver phenotype in MC4R-KO mice. Indeed, deficiency of leptin signaling protects against hepatic fibrosis in several rodent models of chronic liver injury.^{9–11} Exogenous leptin administration also accelerates carbon tetrachloride-induced liver fibrosis in WT mice.⁴⁵ These findings led us to speculate that leptin acts as a pro-inflammatory and pro-fibrotic cytokine in liver fibrosis. However, obesity is associated with the reduced ability of circulating leptin to regulate energy homeostasis or central leptin resistance.⁴⁶ Inasmuch as leptin receptors are widely expressed in peripheral tissues including the liver,⁴⁷ leptin may act directly on the liver to induce inflammation and fibrosis. If so, it would be important to know whether leptin is effective in the peripheral tissues in obesity. Further studies will be required to elucidate how hyperleptinemia is involved in development of the hepatic phenotype in MC4R-KO mice. It would be interesting to generate tissue-specific leptin receptor-deficient mice and/or MC4R-KO mice crossed with *ob/ob* mice for the next phase of study.

In conclusion, the present study is the first to demonstrate that MC4R-KO mice develop a liver condition similar to human NASH when fed an HFD, which is associated with obesity, insulin resistance, and dyslipidemia. Of

note, they develop well-differentiated HCC after long-term HFD feeding. Our data support the concept that NASH develops from a combination of excessive lipid accumulation in the liver and systemic and/or local chronic inflammation. Thus, MC4R-KO mice would provide a novel mouse model of NASH with which to investigate the sequence of events that make up diet-induced hepatic steatosis, liver fibrosis, and HCC, and thus aid in understanding its pathophysiologic features, pursuing specific biomarkers, and evaluating potential therapeutic strategies.

Acknowledgments

We thank Dr. Joel K. Elmquist (University of Texas Southwestern Medical Center, Dallas, TX) for the gift of MC4R-KO mice, Dr. Snorri Thorgeirsson (National Institutes of Health, Bethesda, MD) for helpful comments, Ai Togo for secretarial assistance, Takahiro Fukaishi for technical assistance, and the members of the Ogawa Laboratory for helpful discussions.

References

1. Neuschwander-Tetri BA, Caldwell SH: Nonalcoholic steatohepatitis: summary of an AASLD single topic conference. *Hepatology* 2003, 37:1202–1219
2. Marchesini G, Bugianesi E, Forlani G, Cerrelli F, Lenzi M, Manini R, Natale S, Vanni E, Villanova N, Melchionda N, Rizzetto M: Nonalcoholic fatty liver, steatohepatitis, and the metabolic syndrome. *Hepatology* 2003, 37:917–923
3. Varela-Rey M, Embade N, Ariz U, Lu SC, Mato JM, Martinez-Chantar ML: Non-alcoholic steatohepatitis and animal models: understanding the human disease. *Int J Biochem Cell Biol* 2009, 41:969–976
4. Day CP, James OF: Steatohepatitis: a tale of two "hits"? *Gastroenterology* 1998, 114:842–845
5. Browning JD, Horton JD: Molecular mediators of hepatic steatosis and liver injury. *J Clin Invest* 2004, 114:147–152
6. Neuschwander-Tetri BA: Hepatic lipotoxicity and the pathogenesis of nonalcoholic steatohepatitis: the central role of nontriglyceride fatty acid metabolites. *Hepatology* 2010, 52:774–788
7. Day CP: From fat to inflammation. *Gastroenterology* 2006, 130:207–210
8. Marra F, Bertolani C: Adipokines in liver diseases. *Hepatology* 2009, 50:957–969
9. Leclercq IA, Farrell GC, Schriemer R, Robertson GR: Leptin is essential for the hepatic fibrogenic response to chronic liver injury. *J Hepatol* 2002, 37:206–213
10. Aleffi S, Petrai I, Bertolani C, Parola M, Colombatto S, Novo E, Vizzutti F, Anania FA, Milani S, Rombouts K, Laffi G, Pinzani M, Marra F: Upregulation of proinflammatory and proangiogenic cytokines by leptin in human hepatic stellate cells. *Hepatology* 2005, 42:1339–1348
11. Saxena NK, Ikeda K, Rockey DC, Friedman SL, Anania FA: Leptin in hepatic fibrosis: evidence for increased collagen production in stellate cells and lean littermates of *ob/ob* mice. *Hepatology* 2002, 35:762–771
12. Kamada Y, Matsumoto H, Tamura S, Fukushima J, Kiso S, Fukui K, Igura T, Maeda N, Kihara S, Funahashi T, Matsuzawa Y, Shimomura I, Hayashi N: Hypoadiponection accelerates hepatic tumor formation in a nonalcoholic steatohepatitis mouse model. *J Hepatol* 2007, 47:556–564
13. Balthasar N, Dalgaard LT, Lee CE, Yu J, Funahashi H, Williams T, Ferreira M, Tang V, McGovern RA, Kenny CD, Christiansen LM, Edelstein E, Choi B, Boss O, Aschkenasi C, Zhang CY, Mountjoy K, Kishi T, Elmquist JK, Lowell BB: Divergence of melanocortin pathways in the control of food intake and energy expenditure. *Cell* 2005, 123:493–505

14. Vaisse C, Clement K, Durand E, Hercberg S, Guy-Grand B, Froguel P: Melanocortin-4 receptor mutations are a frequent and heterogeneous cause of morbid obesity. *J Clin Invest* 2000, 106:253–262
15. Friedman JM, Halaas JL: Leptin and the regulation of body weight in mammals. *Nature* 1998, 395:763–770
16. Marsh DJ, Hloppeter G, Huszar D, Laufer R, Yagaloff KA, Fisher SL, Burn P, Palmiter RD: Response of melanocortin-4 receptor-deficient mice to anorectic and orexigenic peptides. *Nat Genet* 1999, 21:119–122
17. Huszar D, Lynch CA, Fairchild-Huntress V, Dunmore JH, Fang Q, Berkemeier LR, Gu W, Kesterson RA, Boston BA, Cone RD, Smith FJ, Campfield LA, Burn P, Lee F: Targeted disruption of the melanocortin-4 receptor results in obesity in mice. *Cell* 1997, 88:131–141
18. Albarado DC, McClaine J, Stephens JM, Mynatt RL, Ye J, Bannon AW, Richards WG, Butler AA: Impaired coordination of nutrient intake and substrate oxidation in melanocortin-4 receptor knockout mice. *Endocrinology* 2004, 145:243–252
19. Sutton GM, Trevaskis JL, Hulver MW, McMillan RP, Markward NJ, Babin MJ, Meyer EA, Butler AA: Diet-genotype interactions in the development of the obese, insulin-resistant phenotype of C57BL/6J mice lacking melanocortin-3 or -4 receptors. *Endocrinology* 2006, 147:2183–2196
20. Sakaida I, Terai S, Yamamoto N, Aoyama K, Ishikawa T, Nishina H, Okita K: Transplantation of bone marrow cells reduces CCl4-induced liver fibrosis in mice. *Hepatology* 2004, 40:1304–1311
21. Tanaka M, Suganami T, Sugita S, Shimoda Y, Kasahara M, Aoe S, Takeya M, Takeda S, Kamei Y, Ogawa Y: Role of central leptin signaling in renal macrophage infiltration. *Endocr J* 2010, 57:61–72
22. Kitagawa K, Wada T, Furuichi K, Hashimoto H, Ishiwata Y, Asano M, Takeya M, Kuziel WA, Matsushima K, Mukaida N, Yokoyama H: Blockade of CCR2 ameliorates progressive fibrosis in kidney. *Am J Pathol* 2004, 165:237–246
23. Itoh M, Suganami T, Satoh N, Tanimoto-Koyama K, Yuan X, Tanaka M, Kawano H, Yano T, Aoe S, Takeya M, Shimatsu A, Kuzuya H, Kamei Y, Ogawa Y: Increased adiponectin secretion by highly purified eicosapentaenoic acid in rodent models of obesity and human obese subjects. *Arterioscler Thromb Vasc Biol* 2007, 27:1918–1925
24. Juluri R, Vuppalanchi R, Olson J, Unalp A, Van Natta ML, Cummings OW, Tonascia J, Chalasani N: Generalizability of the Nonalcoholic Steatohepatitis Clinical Research Network Histologic Scoring System for Nonalcoholic Fatty Liver Disease. *J Clin Gastroenterol* 2010, 45: 55–58
25. Kondo K, Shibata R, Unno K, Shimano M, Ishii M, Kito T, Shintani S, Walsh K, Ouchi N, Murohara T: Impact of a single intracoronary administration of adiponectin on myocardial ischemia/reperfusion injury in a pig model. *Circ Cardiovasc Interv* 2010, 3:166–173
26. Deushi M, Nomura M, Kawakami A, Haraguchi M, Ito M, Okazaki M, Ishii H, Yoshida M: Ezetimibe improves liver steatosis and insulin resistance in obese rat model of metabolic syndrome. *FEBS Lett* 2007, 581:5664–5670
27. Marra F, Gastaldelli A, Svegliati Baroni G, Tell G, Tiribelli C: Molecular basis and mechanisms of progression of non-alcoholic steatohepatitis. *Trends Mol Med* 2008, 14:72–81
28. Weisberg SP, McCann D, Desai M, Rosenbaum M, Leibel RL, Ferrante AW Jr: Obesity is associated with macrophage accumulation in adipose tissue. *J Clin Invest*. 2003;112:1796–1808
29. Unger RH, Scherer PE: Gluttony, sloth and the metabolic syndrome: a roadmap to lipotoxicity. *Trends Endocrinol Metab* 2010, 21:345–352
30. DeLeve LD, Wang X, Kanel GC, Atkinson RD, McCuskey RS: Prevention of hepatic fibrosis in a murine model of metabolic syndrome with nonalcoholic steatohepatitis. *Am J Pathol* 2008, 173:993–1001
31. Ito M, Suzuki J, Tsujioaka S, Sasaki M, Gomori A, Shirakura T, Hirose H, Ito M, Ishihara A, Iwaasa H, Kanatani A: Longitudinal analysis of murine steatohepatitis model induced by chronic exposure to high-fat diet. *Hepatol Res* 2007, 37:50–57
32. Larter CZ, Yeh MM, Van Rooyen DM, Teoh NC, Brooling J, Hou JY, Williams J, Clyne M, Nolan CJ, Farrell GC: Roles of adipose restriction and metabolic factors in progression of steatosis to steatohepatitis in obese, diabetic mice. *J Gastroenterol Hepatol* 2009, 24:1658–1668
33. Martinez-Chantar ML, Corrales FJ, Martinez-Cruz LA, Garcia-Trevijano ER, Huang ZZ, Chen L, Kanel G, Avila MA, Mato JM, Lu SC: Spontaneous oxidative stress and liver tumors in mice lacking methionine adenosyltransferase 1A. *FASEB J* 2002, 16:1292–1294
34. Horie Y, Suzuki A, Kataoka E, Sasaki T, Hamada K, Sasaki J, Mizuno K, Hasegawa G, Kishimoto H, Iizuka M, Naito M, Enomoto K, Watanabe S, Mak TW, Nakano T: Hepatocyte-specific Pten deficiency results in steatohepatitis and hepatocellular carcinomas. *J Clin Invest* 2004, 113:1774–1783
35. Park EJ, Lee JH, Yu GY, He G, Ali SR, Holzer RG, Osterreicher CH, Takahashi H, Karin M: Dietary and genetic obesity promote liver inflammation and tumorigenesis by enhancing IL-6 and TNF expression. *Cell* 2010, 140:197–208
36. Suganami T, Nishida J, Ogawa Y: A paracrine loop between adipocytes and macrophages aggravates inflammatory changes: role of free fatty acids and tumor necrosis factor α . *Arterioscler Thromb Vasc Biol* 2005, 25:2062–2068
37. Suganami T, Tanimoto-Koyama K, Nishida J, Itoh M, Yuan X, Mizuarai S, Kotani H, Yamaoka S, Miyake K, Aoe S, Kamei Y, Ogawa Y: Role of the Toll-like receptor 4/NF- κ B pathway in saturated fatty acid-induced inflammatory changes in the interaction between adipocytes and macrophages. *Arterioscler Thromb Vasc Biol* 2007, 27:84–91
38. Khan T, Muise ES, Iyengar P, Wang ZV, Chandalia M, Abate N, Zhang BB, Bonaldo P, Chua S, Scherer PE: Metabolic dysregulation and adipose tissue fibrosis: role of collagen VI. *Mol Cell Biol* 2009, 29: 1575–1591
39. Divoux A, Tordjman J, Lacasa D, Veyrie N, Hugol D, Aissat A, Basdevant A, Guerre-Millo M, Poitou C, Zucker JD, Bedossa P, Clement K: Fibrosis in human adipose tissue: composition, distribution, and link with lipid metabolism and fat mass loss. *Diabetes* 2010, 59:2817–2825
40. McQuaid SE, Hodson L, Neville MJ, Dennis AL, Cheeseman J, Humphreys SM, Ruge T, Gilbert M, Fielding BA, Frayn KN, Karpe F: Downregulation of adipose tissue fatty acid trafficking in obesity: a driver for ectopic fat deposition? *Diabetes* 2011, 60:47–55
41. Gautron L, Lee C, Funahashi H, Friedman J, Lee S, Elmquist J: Melanocortin-4 receptor expression in a vago-vagal circuitry involved in postprandial functions. *J Comp Neurol* 2010, 518:6–24
42. Nogueiras R, Wiedmer P, Perez-Tilve D, Veyrat-Durebex C, Keogh JM, Sutton GM, Pfluger PT, Castaneda TR, Neschen S, Hofmann SM, Howles PN, Morgan DA, Benoit SC, Szanto I, Schrott B, Schurmans A, Joost HG, Hammond C, Hui DY, Woods SC, Rahmouni K, Butler AA, Farooqi IS, O'Rahilly S, Rohner-Jeanrenaud F, Tschöp MH: The central melanocortin system directly controls peripheral lipid metabolism. *J Clin Invest* 2007, 117:3475–3488
43. Inoue H, Ogawa W, Asakawa A, Okamoto Y, Nishizawa A, Matsumoto M, Teshigawara K, Matsuki Y, Watanabe E, Hiramatsu R, Notohara K, Katayose K, Okamura H, Kahn CR, Noda T, Takeda K, Akira S, Inui A, Kasuga M: Role of hepatic STAT3 in brain-insulin action on hepatic glucose production. *Cell Metab* 2006, 3:267–275
44. Uno K, Katagiri H, Yamada T, Ishigaki Y, Ogihara T, Imai J, Hasegawa Y, Gao J, Kaneko K, Iwasaki H, Ishihara H, Sasano H, Inukai K, Mizuguchi H, Asano T, Shiota M, Nakazato M, Oka Y: Neuronal pathway from the liver modulates energy expenditure and systemic insulin sensitivity. *Science* 2006, 312:1656–1659
45. Ikejima K, Honda H, Yoshikawa M, Hirose M, Kitamura T, Takei Y, Sato N: Leptin augments inflammatory and profibrogenic responses in the murine liver induced by hepatotoxic chemicals. *Hepatology* 2001, 34:288–297
46. Friedman JM: Modern science versus the stigma of obesity. *Nat Med* 2004, 10:563–569
47. Morris DL, Rui L: Recent advances in understanding leptin signaling and leptin resistance. *Am J Physiol Endocrinol Metab* 2009, 297: E1247–E1259

Review Article

Adipose Tissue Remodeling as Homeostatic Inflammation

Michiko Itoh,¹ Takayoshi Suganami,¹ Rumi Hachiya,¹ and Yoshihiro Ogawa^{1,2}

¹ Department of Molecular Medicine and Metabolism, Medical Research Institute, Tokyo Medical and Dental University, 1-5-45 Yushima, Bunkyo-ku, Tokyo 113-8510, Japan

² Global Center of Excellence Program, International Research Center for Molecular Science in Tooth and Bone Diseases, Tokyo Medical and Dental University, Tokyo 113-8510, Japan

Correspondence should be addressed to Yoshihiro Ogawa, ogawa.mmm@mri.tmd.ac.jp

Received 23 March 2011; Accepted 27 April 2011

Academic Editor: Ichiro Manabe

Copyright © 2011 Michiko Itoh et al. This is an open access article distributed under the Creative Commons Attribution License, which permits unrestricted use, distribution, and reproduction in any medium, provided the original work is properly cited.

Evidence has accumulated indicating that obesity is associated with a state of chronic, low-grade inflammation. Obese adipose tissue is characterized by dynamic changes in cellular composition and function, which may be referred to as “adipose tissue remodeling”. Among stromal cells in the adipose tissue, infiltrated macrophages play an important role in adipose tissue inflammation and systemic insulin resistance. We have demonstrated that a paracrine loop involving saturated fatty acids and tumor necrosis factor- α derived from adipocytes and macrophages, respectively, aggravates obesity-induced adipose tissue inflammation. Notably, saturated fatty acids, which are released from hypertrophied adipocytes via the macrophage-induced lipolysis, serve as a naturally occurring ligand for Toll-like receptor 4 complex, thereby activating macrophages. Such a sustained interaction between endogenous ligands derived from parenchymal cells and pathogen sensors expressed in stromal immune cells should lead to chronic inflammatory responses ranging from the basal homeostatic state to diseased tissue remodeling, which may be referred to as “homeostatic inflammation”. We, therefore, postulate that adipose tissue remodeling may represent a prototypic example of homeostatic inflammation. Understanding the molecular mechanism underlying homeostatic inflammation may lead to the identification of novel therapeutic strategies to prevent or treat obesity-related complications.

1. Introduction

The metabolic syndrome is a constellation of visceral fat obesity, insulin resistance, atherogenic dyslipidemia, and hypertension, which all independently increase the risk of atherosclerotic diseases [1–5]. The adipose tissue secretes a number of bioactive substances or adipocytokines, and unbalanced production of pro- and anti-inflammatory adipocytokines in obese adipose tissue may critically contribute to many aspects of the metabolic syndrome [1–5]. Obesity is now viewed as a state of systemic, chronic low-grade inflammation [1–4]. In contrast to acute inflammation which resolves by an active termination program, chronic inflammation may involve persistent stress and/or impaired resolution process, thereby resulting in functional maladaptation and tissue remodeling [6]. On the other hand, during the course of obesity, adipose tissue is characterized by adipocyte hypertrophy, followed by increased angiogenesis, immune cell infiltration, and extracellular matrix overproduction

[1, 2, 7, 8], which may be referred to as adipose tissue remodeling.

Pathogen sensors or pattern-recognition receptors (PRRs), which are important for the recognition of pathogen-associated molecular patterns (PAMPs) in innate immunity, are also capable of recognizing endogenous ligands, damage-associated molecular patterns (DAMPs) or danger signals (Figure 1) [6, 9, 10]. Interaction between endogenous ligands and pathogen sensors may play a role in the basal homeostatic state as well as diseased tissue remodeling, which has been referred to as homeostatic inflammation [6, 11]. This paper summarizes the molecular mechanism and pathophysiological implication of adipose tissue remodeling as a prototypic example of homeostatic inflammation.

2. Adipose Tissue Inflammation and Adipose Tissue Remodeling

In addition to lipid-laden mature adipocytes, the adipose tissue is composed of various stromal cells, including

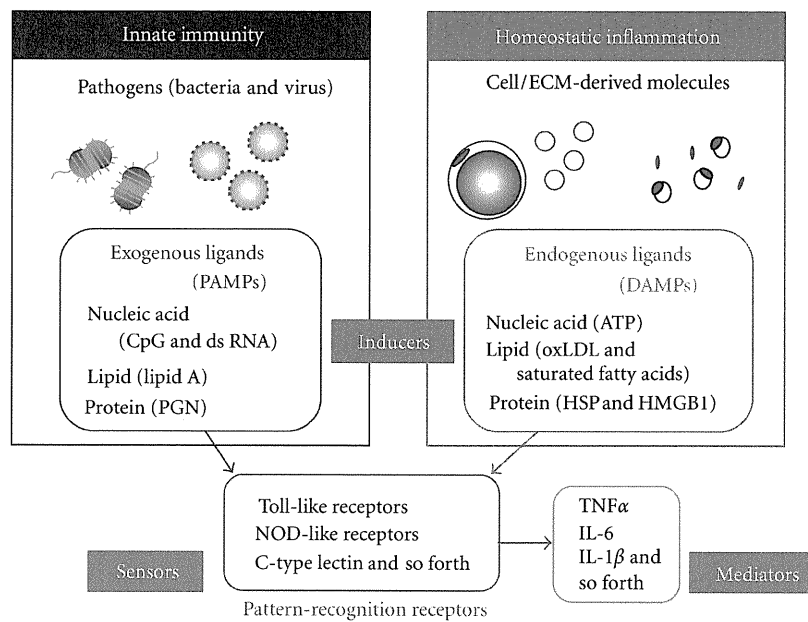


FIGURE 1: Adipose tissue inflammation as homeostatic inflammation. In innate immunity, exogenous ligands (pathogen-associated molecular patterns; PAMPs) are sensed by pattern-recognition receptors (PRRs), thereby inducing inflammatory changes. On the other hand, damage-associated molecular patterns (DAMPs) released from damaged or stressed cells and tissues can activate PRRs, thereby inducing homeostatic inflammation ranging from the basal homeostatic state to diseased tissue remodeling. For instance, free fatty acids (FFAs) released from hypertrophied adipocytes can report, as a danger signal, their diseased state to macrophages via Toll-like receptor 4 (TLR4) complex during the course of obesity. dsRNA, double-strand RNA; PGN, peptidoglycan; ATP, adenosine tri-phosphate; oxLDL, oxidized low-density lipoprotein; HSP, heat shock protein; HMGB1, high-mobility group box-1.

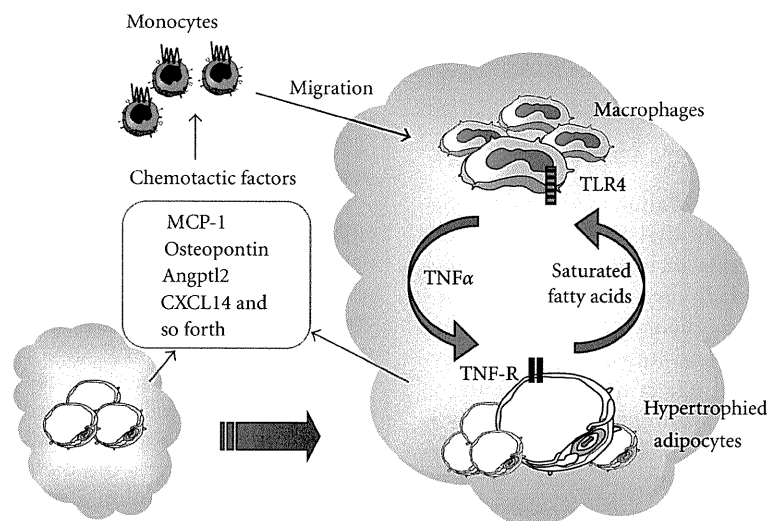


FIGURE 2: Molecular mechanism underlying adipose tissue inflammation. During the course of obesity, adipose tissue secretes several chemotactic factors to induce macrophage infiltration into adipose tissue. Circulating monocytes migrate and infiltrate into adipose tissue through adhesion process to endothelial cells. Macrophages enhance the inflammatory changes through the crosstalk with parenchymal adipocytes. For example, the macrophage-derived tumor necrosis factor- α (TNF α) induces the release of saturated fatty acids from adipocytes via lipolysis, which, in turn, induces inflammatory changes in macrophages via TLR4. Such a paracrine loop between adipocytes and macrophages constitutes a vicious cycle, thereby further accelerating adipose tissue inflammation. TNF-R, TNF α receptor.

preadipocytes, endothelial cells, fibroblasts, and immune cells [12]. Obese adipose tissue exhibits functional and morphological changes, thereby leading to unbalanced production of pro- and anti-inflammatory adipocytokines [1, 2, 7, 8]. The morphological changes found in obese adipose tissue are reminiscent of the chronic inflammatory responses in atherosclerotic vascular walls termed vascular remodeling, which arise from the complex interactions among vascular endothelial cells, vascular smooth muscle cells, lymphocytes, and monocyte-derived macrophages [4]. Vascular remodeling is considered to be an adaptive process in response to long-term changes in hemodynamic conditions and lipid metabolism, thereby contributing to the pathophysiology of vascular diseases [13]. Thus, the dynamic changes seen in obese adipose tissue can be referred to as adipose tissue remodeling. Notably, macrophage infiltration and inflammation-related gene expression in the adipose tissue precedes the development of insulin resistance in animal models [14, 15], suggesting that macrophages should play a central role in adipose tissue remodeling. It is, therefore, important to know the pathophysiologic role of macrophages infiltrated into the adipose tissue during the course of adipose tissue remodeling.

3. Macrophage Infiltration into Obese Adipose Tissue

Evidence has accumulated that adipocytes *per se* secrete pro-inflammatory cytokines and chemokines, such as tumor necrosis factor- α (TNF α), interleukin-6 (IL-6), and monocyte chemoattractant protein-1 (MCP-1), during the course of adipocyte hypertrophy [1–3]. Increased production of chemokines in obese adipose tissue has been implicated in the regulation of monocyte recruitment to adipose tissue [14]. The involvement of MCP-1/chemokine receptor 2 (CCR2) pathway has been extensively studied as the mechanism underlying macrophage infiltration into obese adipose tissue (Figure 2) [16–19]. Moreover, several reports have suggested the role of other chemotactic factors in obesity-induced macrophage infiltration: osteopontin, angiopoietin-like protein 2 (Angptl2), and CXC motif chemokine ligand-14 (CXCL14) (Figure 2) [20–22]. Inhibition of macrophage infiltration into obese adipose tissue through genetic and/or pharmacologic strategies has improved the dysregulation of adipocytokine production, thereby leading to the amelioration of obesity-induced adipose tissue inflammation and insulin resistance. Indeed, macrophage infiltration and inflammation-related gene expression in the adipose tissue precedes the development of insulin resistance in animal models [14, 15]. Understanding the molecular mechanisms underlying increased macrophage infiltration into obese adipose tissue may lead to the identification of novel therapeutic strategies to prevent or treat obesity-induced adipose tissue inflammation.

4. Interaction between Adipocytes and Macrophages

The adipose tissue macrophages also represent a major source of pro-inflammatory cytokines, which play important roles in chronic inflammatory responses in obese adipose tissue. Using an *in vitro* coculture system composed of adipocytes and macrophages, we have demonstrated that a paracrine loop involving saturated fatty acids and TNF α derived from adipocytes and macrophages, respectively, establishes a vicious cycle that augments the inflammatory changes (Figure 2) [23]. Among numerous cytokines derived from infiltrated macrophages in obese adipose tissue, TNF α acts on TNF receptor in hypertrophied adipocytes, thereby inducing pro-inflammatory cytokine production and adipocyte lipolysis via nuclear factor- κ B- (NF- κ B-) dependent and independent (possibly mitogen-activated protein kinase- (MAPK-) dependent) mechanisms, respectively [24]. On the other hand, saturated fatty acids released from adipocytes serve as a naturally occurring ligand for Toll-like receptor 4 (TLR4) complex, which is essential for the recognition of lipopolysaccharide (LPS), to induce NF- κ B activation in macrophages [24].

The interaction between adipocytes and macrophages results in marked upregulation of pro-inflammatory adipocytokines and significant downregulation of anti-inflammatory adipocytokines, which lead to development of obesity-related complications in multiple organs, such as atherosclerosis and hepatic steatosis [1–4]. For instance, adiponectin is a well-established anti-inflammatory adipocytokine, which is markedly downregulated in obese adipose tissue, and supplementation of adiponectin in obese mice effectively reverses insulin resistance in the skeletal muscle and liver [25, 26]. On the other hand, overproduction of MCP-1 induces macrophage infiltration into the adipose tissue and directly induces insulin resistance in the skeletal muscle and liver [17, 18, 27]. Thus, dysregulation of adipocytokine production as a result of inflammatory changes in the adipose tissue may be involved in the pathogenesis of metabolic derangements in obesity.

5. Heterogeneity of Adipose Tissue Macrophages

Recent studies have pointed to the phenotypic change of macrophages in lean and obese adipose tissue; M1 or classically activated (pro-inflammatory) macrophages and M2 or alternatively activated (anti-inflammatory) macrophages (Figure 3) [28]. Adipocytes in lean adipose tissue produce humoral factors that induce M2 activation of macrophages, such as interleukin-4 (IL-4) and interleukin-13 (IL-13), and M2 activated macrophages release anti-inflammatory mediators, such as interleukin (IL-10) [29]. On the other hand, hypertrophied adipocytes secrete pro-inflammatory saturated fatty acids, cytokines, and chemokines to induce M1 polarization of macrophages [29]. Activated M1 macrophages in turn produce pro-inflammatory cytokines and

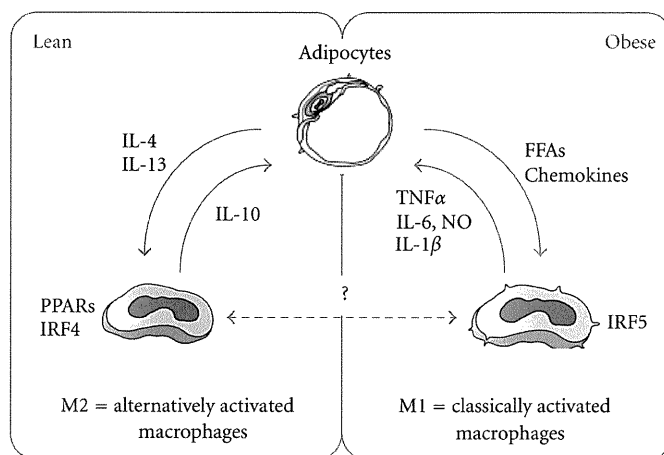


FIGURE 3: Regulation of macrophage polarity in adipose tissue. Recent evidence has also pointed to the heterogeneity of adipose tissue macrophages, that is, M1 or classically activated (pro-inflammatory) macrophages and M2 or alternatively activated (anti-inflammatory) macrophages. Under lean condition, adipocytes secrete factors that promote M2 activation of macrophages, such as interleukin-4 (IL) and interleukin-13 (IL-13). M2 macrophages secrete anti-inflammatory mediators. On the other hand, adipocytes secrete pro-inflammatory FFAs, chemokines, and cytokines under obese condition. Activated M1 macrophages produce large amounts of pro-inflammatory cytokines, thereby accelerating inflammatory responses in adipose tissue through paracrine interaction between adipocytes and macrophages.

chemokines, thereby accelerating adipose tissue inflammation.

We have recently identified activating transcription factor 3 (ATF3), a member of ATF/cAMP response element-binding protein family of basic leucine zipper-type transcription factors, as a target gene of saturated fatty acids/TLR4 signaling in adipose tissue macrophages and found that ATF3 attenuates obesity-induced macrophage activation in obese adipose tissue [30]. On the other hand, peroxisome proliferator-activated receptor γ (PPAR γ) and peroxisome proliferator-activated receptor β/δ (PPAR β/δ) can stimulate M2 polarization of adipose tissue macrophages and thus systemic insulin sensitivity [31–34]. Indeed, the activation of PPAR γ by pioglitazone, a thiazolidinedione class of insulin sensitizer, improves the unbalanced M1/M2 phenotype of adipose tissue macrophages in diet-induced obese mice [35]. Interestingly, circulating blood monocytes, precursors of infiltrated macrophages to the site of chronic inflammation, also express both M1 and M2 markers [36, 37]. Moreover, monocytes in obese mice and/or obese type 2 diabetic patients show significantly higher expression of M1 markers and lower expression of M2 markers relative to normal-weight controls [36]. Thus, pioglitazone treatment improves the unbalanced M1/M2 phenotype of monocytes, which may contribute to its antidiabetic and antiatherogenic effect [36, 37].

Recent studies have found other molecules that regulate macrophage polarization; that is, Jumonji domain containing-3 (Jmjd3) is essential for M2 activation through demethylation of interferon-regulatory factor 4 (IRF4) under infectious condition [38], and interferon-regulatory factor 5 (IRF5) is crucial for conversion from M2 to M1 activation in response to LPS [39]. It is interesting to know their importance in the regulation of macrophage polarization and plasticity during the course of obesity. Modulating macrophage

activation state in obese adipose tissue would be a novel therapeutic target to treat or prevent the progression of obesity-induced complications such as diabetes and atherosclerosis.

6. Adipose Tissue Remodeling and Ectopic Lipid Accumulation

The adipose tissue is primarily an energy reservoir that stores fatty acids in the form of triglyceride, which is facilitated by insulin. However, obesity induces insulin-resistant state and inflammation in the adipose tissue, both of which lead to increased fatty acid release from the adipose tissue [1, 23, 29]. Moreover, recent studies have suggested that increased expression of genes related to ECM components and fibrotic changes in the adipose tissue from obese subjects and animals [40–43]. It is reported that adipose tissue fibrosis is negatively correlated with adipocyte diameters in human adipose tissue [44], suggesting that increased ECM components may limit adipose tissue expandability. Indeed, Khan et al. reported that mice lacking collagen VI, which is expressed predominantly in the adipose tissue, exhibit the uninhibited adipose tissue expansion and substantial improvements in whole-body energy homeostasis during a high-fat diet feeding [43]. It is conceivable that the rigid extracellular environment limits adipocyte expansion, and triggers adipocyte cell death and inflammatory responses through MAPK activation by increased shear stress and membrane stretching [43, 44]. Recent evidence suggests that impaired lipid storage in the adipose tissue may contribute to ectopic lipid accumulation in the skeletal muscle, liver, and pancreatic β -cells, where lipotoxicity impairs their metabolic functions [45–47]. This discussion supports the emerging view that metabolic problems associated with obesity become overt when adipose tissue cannot fully meet demands for

additional lipid storage in addition to the dysregulation of adipocytokine production.

7. Adipose Tissue Remodeling as Homeostatic Inflammation

TLR4 is a pattern-recognition receptor essential for the recognition of LPS, which is reported to play an important role in obesity-induced adipose tissue inflammation and systemic glucose and lipid metabolism *in vivo* [24, 48–50]. In obese adipose tissue, TLR4 expressed in macrophages is capable of sensing saturated fatty acids (FAs) released from adipocytes to induce chronic inflammatory responses [24, 51, 52], suggesting that saturated fatty acids could be a danger signal. On the other hand, free fatty acids (FFAs) are an important energy source mobilized from triglycerides stored in the adipose tissue, particularly under starvation conditions. Kosteli et al. have recently suggested that FFAs released from adipocytes during fasting recruit macrophages into the adipose tissue, which may be involved in the regulation of local lipid concentrations [53]. In this regard, FFAs, when released physiologically during fasting or starvation via adipocyte lipolysis, may be involved in the regulation of metabolic homeostasis within the adipose tissue rather than a danger signal. Under overnutrition conditions, increased concentrations of FFAs also activate inflammatory pathways to maintain adipose tissue homeostasis such as tissue repair and regulation of metabolism. When cellular and/or tissue stresses are excessive and/or sustained and adaptive responses are no longer possible, inflammatory responses are prolonged (i.e., chronic inflammation), thereby leading to diseased tissue remodeling [6].

Recently, we have reported that macrophage-inducible C-type lectin (Mincle; also called Clec4e and Clec5f9), a pathogen sensor for pathogenic fungi and *Mycobacterium tuberculosis*, is induced in adipose tissue macrophages in obesity at least partly through the saturated fatty acid/TLR4/NF- κ B pathway, thereby suggesting its pathophysiological role in obesity-induced adipose tissue inflammation [54]. Yamasaki et al. reported that Mincle serves as a receptor for SAP130, a component of small nuclear ribonucleoprotein released from damaged cells, to sense cell death and induce pro-inflammatory cytokine production [55]. Since dead adipocytes are surrounded by macrophages in the adipose tissue of obese humans and mice (crown-like structure) [7, 8, 56], it is conceivable that Mincle plays a role in sensing adipocyte-derived endogenous ligand(s) during adipocyte death.

The above discussion supports the concept that interaction between endogenous ligands and pathogen sensors in the adipose tissue involves multiple stages of adipose tissue remodeling, ranging from normal metabolic homeostasis to diseased tissue remodeling, which may be referred to as homeostatic inflammation. It is interesting to identify other endogenous danger signals and pathogen sensors that contribute to the pathophysiology of adipose tissue inflammation.

8. Homeostatic Inflammation and Other Metabolic Disorders

Recent evidence has provided new insight into the interaction between endogenous ligands and pathogen sensors in a variety of chronic inflammatory diseases such as atherosclerosis, diabetes mellitus, malignant cancers, autoimmune diseases, and even neurodegenerative diseases. Similar to the interaction between saturated fatty acids and TLR4, oxidized low-density lipoprotein (LDL), known as a ligand for the scavenger receptor CD36, is reported to trigger inflammatory signaling through a newly identified heterodimer of TLR4 and TLR6 in macrophages [57] and also to trigger CD36-TLR2-dependent apoptosis in macrophages under endoplasmic reticulum stress [58]. On the other hand, Schulthess et al. reported that CXC motif chemokine ligand-10 (CXCL10), when upregulated in diabetic pancreatic islet, is capable of binding to TLR4 in β cells in pancreatic islets to induce apoptosis [59].

In Nod-like receptor family, the NACHT, LRR, and PYD domain-containing protein 3 (NLRP3) inflammasome is well characterized. The NLRP3 inflammasome is a cytosolic protein complex consisting of the regulatory subunit NLRP3, the adaptor protein apoptosis-associated speck-like protein containing a caspase-recruitment domain (ASC) and the effector subunit caspase-1. It is activated by pathogen-derived DNA and endogenous DAMPs such as components of necrotic cells and damaged tissues [60, 61]. Several lines of evidence have suggested that the NLRP3 inflammasome plays an important role in the pathogenesis of obesity-related diseases. NLRP3 deficient mice show improved glucose tolerance and insulin sensitivity [62]. It is also reported that ceramide and islet amyloid polypeptide (IAPP) activate as danger signals for NLRP3 inflammasome in adipose tissue macrophages and pancreatic islets, respectively, which results in insulin resistance [63–65]. In atherogenesis, it is reported that crystalline cholesterol acts as an endogenous danger signal and its deposition in arteries or elsewhere is an early cause rather than a late consequence of inflammation [66]. A better understanding of the molecular basis underlying homeostatic inflammation would allow more efficient multidisciplinary approach to and a better assessment of the metabolic syndrome.

9. Concluding Remarks

Obesity may be viewed as a chronic low-grade inflammation as well as a metabolic disease. Although considerable progress has been made in understanding the cellular and molecular events that are involved in acute inflammation caused by infection, there is no clear understanding of their physiological counterpart of the systemic chronic inflammatory state, which could be referred as homeostatic inflammation. The interaction between parenchymal and stromal cells through a number of endogenous ligands and pathogen sensors may contribute to inflammatory responses in obese adipose tissue as well as other metabolic organs. Understanding

the molecular mechanism underlying adipose tissue remodeling as homeostatic inflammation may lead to novel therapeutic strategies to prevent or treat obesity-related complications.

Abbreviations

Angptl2:	Angiopoietin-like protein 2
ASC:	Apoptosis-associated speck-like protein containing a caspase-recruitment domain
ATF3:	Activating transcription factor 3
CCR2:	Chemokine receptor 2
CXCL10:	CXC motif chemokine ligand-10
CXCL14:	CXC motif chemokine ligand-14
DAMP:	Damage-associated molecular pattern
ECM:	Extracellular matrix
FFA:	Free fatty acid
IAPP:	Islet amyloid polypeptide
IL-4:	Interleukin-4
IL-6:	Interleukin-6
IL-10:	Interleukin-10
IL-13:	Interleukin-13
IRF4:	Interferon-regulatory factor 4
IRF5:	Interferon-regulatory factor 5
Jmjd3:	Jumonji domain containing-3
LDL:	Low-density lipoprotein
LPS:	Lipopolysaccharide
MAPK:	Mitogen-activated protein kinase
MCP-1:	Monocyte chemoattractant protein-1
NF- κ B:	Nuclear factor- κ B
NLRP3:	NACHT, LRR and PYD domain-containing protein 3
PAMP:	Pathogen-associated molecular pattern
PPAR γ :	Peroxisome proliferator-activated receptor γ
PPAR β/δ :	Peroxisome proliferator-activated receptor β/δ
PRR:	Pattern-recognition receptor
SVF:	Stromal vascular fraction
TLR4:	Toll-like receptor 4
TNF α :	Tumor necrosis factor- α .

Acknowledgments

Work in the authors' laboratory was supported in part by a Grant-in-Aid for Scientific Research from the Ministry of Education, Culture, Sports, Science, and Technology of Japan, and the Ministry of Health, Labor, and Welfare of Japan.

References

- [1] S. Schenk, M. Saberi, and J. M. Olefsky, "Insulin sensitivity: modulation by nutrients and inflammation," *Journal of Clinical Investigation*, vol. 118, no. 9, pp. 2992–3002, 2008.
- [2] G. S. Hotamisligil, "Inflammation and metabolic disorders," *Nature*, vol. 444, no. 7121, pp. 860–867, 2006.
- [3] A. H. Berg and P. E. Scherer, "Adipose tissue, inflammation, and cardiovascular disease," *Circulation Research*, vol. 96, no. 9, pp. 939–949, 2005.
- [4] V. Z. Rocha and P. Libby, "Obesity, inflammation, and atherosclerosis," *Nature Reviews Cardiology*, vol. 6, no. 6, pp. 399–409, 2009.
- [5] Y. Matsuzawa, T. Funahashi, and T. Nakamura, "Molecular mechanism of metabolic syndrome X: contribution of adipocytokines-adipocyte-derived bioactive substances," *Annals of the New York Academy of Sciences*, vol. 892, pp. 146–154, 1999.
- [6] R. Medzhitov, "Origin and physiological roles of inflammation," *Nature*, vol. 454, no. 7203, pp. 428–435, 2008.
- [7] S. Nishimura, I. Manabe, M. Nagasaki et al., "Adipogenesis in obesity requires close interplay between differentiating adipocytes, stromal cells, and blood vessels," *Diabetes*, vol. 56, no. 6, pp. 1517–1526, 2007.
- [8] S. Nishimura, I. Manabe, M. Nagasaki et al., "In vivo imaging in mice reveals local cell dynamics and inflammation in obese adipose tissue," *Journal of Clinical Investigation*, vol. 118, no. 2, pp. 710–721, 2008.
- [9] R. Medzhitov and C. A. Janeway Jr., "Decoding the patterns of self and nonself by the innate immune system," *Science*, vol. 296, no. 5566, pp. 298–300, 2002.
- [10] X. Zhang and D. M. Mosser, "Macrophage activation by endogenous danger signals," *Journal of Pathology*, vol. 214, no. 2, pp. 161–178, 2008.
- [11] T. Suganami and Y. Ogawa, "Adipose tissue macrophages: their role in adipose tissue remodeling," *Journal of Leukocyte Biology*, vol. 88, no. 1, pp. 33–39, 2010.
- [12] F. Wasserman, *Handbook of Physiology*, American Physiology Society, Washington, DC, USA, 1965.
- [13] G. H. Gibbons and V. J. Dzau, "The emerging concept of vascular remodeling," *The New England Journal of Medicine*, vol. 330, no. 20, pp. 1431–1438, 1994.
- [14] S. P. Weisberg, D. McCann, M. Desai, M. Rosenbaum, R. L. Leibel, and A. W. Ferrante Jr., "Obesity is associated with macrophage accumulation in adipose tissue," *Journal of Clinical Investigation*, vol. 112, no. 12, pp. 1796–1808, 2003.
- [15] H. Xu, G. T. Barnes, Q. Yang et al., "Chronic inflammation in fat plays a crucial role in the development of obesity-related insulin resistance," *Journal of Clinical Investigation*, vol. 112, no. 12, pp. 1821–1830, 2003.
- [16] S. P. Weisberg, D. Hunter, R. Huber et al., "CCR2 modulates inflammatory and metabolic effects of high-fat feeding," *Journal of Clinical Investigation*, vol. 116, no. 1, pp. 115–124, 2006.
- [17] H. Kanda, S. Tateya, Y. Tamori et al., "MCP-1 contributes to macrophage infiltration into adipose tissue, insulin resistance, and hepatic steatosis in obesity," *Journal of Clinical Investigation*, vol. 116, no. 6, pp. 1494–1505, 2006.
- [18] N. Kamei, K. Tobe, R. Suzuki et al., "Overexpression of monocyte chemoattractant protein-1 in adipose tissues causes macrophage recruitment and insulin resistance," *Journal of Biological Chemistry*, vol. 281, no. 36, pp. 26602–26614, 2006.
- [19] A. Ito, T. Suganami, A. Yamauchi et al., "Role of CC chemokine receptor 2 in bone marrow cells in the recruitment of macrophages into obese adipose tissue," *Journal of Biological Chemistry*, vol. 283, no. 51, pp. 35715–35723, 2008.
- [20] T. Nomiya, D. Perez-Tilve, D. Ogawa et al., "Osteopontin mediates obesity-induced adipose tissue macrophage infiltration and insulin resistance in mice," *Journal of Clinical Investigation*, vol. 117, no. 10, pp. 2877–2888, 2007.
- [21] N. Nara, Y. Nakayama, S. Okamoto et al., "Disruption of CXC motif chemokine ligand-14 in mice ameliorates obesity-induced insulin resistance," *Journal of Biological Chemistry*, vol. 282, no. 42, pp. 30794–30803, 2007.

- [22] M. Tabata, T. Kadomatsu, S. Fukuhara et al., "Angiopoietin-like protein 2 promotes chronic adipose tissue inflammation and obesity-related systemic insulin resistance," *Cell Metabolism*, vol. 10, no. 3, pp. 178–188, 2009.
- [23] T. Suganami, J. Nishida, and Y. Ogawa, "A paracrine loop between adipocytes and macrophages aggravates inflammatory changes: role of free fatty acids and tumor necrosis factor α ," *Arteriosclerosis, Thrombosis, and Vascular Biology*, vol. 25, no. 10, pp. 2062–2068, 2005.
- [24] T. Suganami, K. Tanimoto-Koyama, J. Nishida et al., "Role of the toll-like receptor 4/NF- κ B pathway in saturated fatty acid-induced inflammatory changes in the interaction between adipocytes and macrophages," *Arteriosclerosis, Thrombosis, and Vascular Biology*, vol. 27, no. 1, pp. 84–91, 2007.
- [25] T. Yamauchi, J. Kamon, H. Waki et al., "The fat-derived hormone adiponectin reverses insulin resistance associated with both lipotrophy and obesity," *Nature Medicine*, vol. 7, no. 8, pp. 941–946, 2001.
- [26] N. Maeda, I. Shimomura, K. Kishida et al., "Diet-induced insulin resistance in mice lacking adiponectin/ACRP30," *Nature Medicine*, vol. 8, no. 7, pp. 731–737, 2002.
- [27] S. Tateya, Y. Tamori, T. Kawaguchi, H. Kanda, and M. Kasuga, "An increase in the circulating concentration of monocyte chemoattractant protein-1 elicits systemic insulin resistance irrespective of adipose tissue inflammation in mice," *Endocrinology*, vol. 151, no. 3, pp. 971–979, 2010.
- [28] C. N. Lumeng, J. L. Bodzin, and A. R. Saltiel, "Obesity induces a phenotypic switch in adipose tissue macrophage polarization," *Journal of Clinical Investigation*, vol. 117, no. 1, pp. 175–184, 2007.
- [29] J. M. Olefsky and C. K. Glass, "Macrophages, inflammation, and insulin resistance," *Annual Review of Physiology*, vol. 72, pp. 219–246, 2010.
- [30] T. Suganami, X. Yuan, Y. Shimoda et al., "Activating transcription factor 3 constitutes a negative feedback mechanism that attenuates saturated fatty acid/toll-like receptor 4 signaling and macrophage activation in obese adipose tissue," *Circulation Research*, vol. 105, no. 1, pp. 25–32, 2009.
- [31] J. I. Odegaard, R. R. Ricardo-Gonzalez, M. H. Goforth et al., "Macrophage-specific PPAR γ controls alternative activation and improves insulin resistance," *Nature*, vol. 447, no. 7148, pp. 1116–1120, 2007.
- [32] J. I. Odegaard, R. R. Ricardo-Gonzalez, A. Red Eagle et al., "Alternative M2 activation of kupffer cells by PPAR δ ameliorates obesity-induced insulin resistance," *Cell Metabolism*, vol. 7, no. 6, pp. 496–507, 2008.
- [33] K. Kang, S. M. Reilly, V. Karabacak et al., "Adipocyte-derived Th2 cytokines and myeloid PPAR δ regulate macrophage polarization and insulin sensitivity," *Cell Metabolism*, vol. 7, no. 6, pp. 485–495, 2008.
- [34] D. Vats, L. Mukundan, J. I. Odegaard et al., "Oxidative metabolism and PGC- β attenuate macrophage-mediated inflammation," *Cell Metabolism*, vol. 4, no. 1, pp. 13–24, 2006.
- [35] S. Fujisaka, I. Usui, A. Bukhari et al., "Regulatory mechanisms for adipose tissue M1 and M2 macrophages in diet-induced obese mice," *Diabetes*, vol. 58, no. 11, pp. 2574–2582, 2009.
- [36] N. Satoh, A. Shimatsu, A. Himeno et al., "Unbalanced M1/M2 phenotype of peripheral blood monocytes in obese diabetic patients: effect of pioglitazone," *Diabetes Care*, vol. 33, no. 1, p. e7, 2010.
- [37] M. A. Bouhlel, B. Derudas, E. Rigamonti et al., "PPAR γ activation primes human monocytes into alternative M2 macrophages with anti-inflammatory properties," *Cell Metabolism*, vol. 6, no. 2, pp. 137–143, 2007.
- [38] T. Satoh, O. Takeuchi, A. Vandenbon et al., "The Jmjd3-Irf4 axis regulates M2 macrophage polarization and host responses against helminth infection," *Nature Immunology*, vol. 11, no. 10, pp. 936–944, 2010.
- [39] T. Krausgruber, K. Blazek, T. Smallie et al., "IRF5 promotes inflammatory macrophage polarization and T(H)1-T(H)17 responses," *Nature Immunology*, vol. 12, no. 3, pp. 231–238, 2011.
- [40] C. Henegar, J. Tordjman, V. Achard et al., "Adipose tissue transcriptomic signature highlights the pathological relevance of extracellular matrix in human obesity," *Genome Biology*, vol. 9, no. 1, Article ID R14, 2008.
- [41] D. M. Mutch, J. Tordjman, V. Pelloux et al., "Needle and surgical biopsy techniques differentially affect adipose tissue gene expression profiles," *The American Journal of Clinical Nutrition*, vol. 89, no. 1, pp. 51–57, 2009.
- [42] J. Liu, A. Divoux, J. Sun et al., "Genetic deficiency and pharmacological stabilization of mast cells reduce diet-induced obesity and diabetes in mice," *Nature Medicine*, vol. 15, no. 8, pp. 940–945, 2009.
- [43] T. Khan, E. S. Muise, P. Iyengar et al., "Metabolic dysregulation and adipose tissue fibrosis: role of collagen VI," *Molecular and Cellular Biology*, vol. 29, no. 6, pp. 1575–1591, 2009.
- [44] A. Divoux, J. Tordjman, D. Lacasa et al., "Fibrosis in human adipose tissue: composition, distribution, and link with lipid metabolism and fat mass loss," *Diabetes*, vol. 59, no. 11, pp. 2817–2825, 2010.
- [45] M. Y. Wang, P. Grayburn, S. Chen, M. Ravazzola, L. Orci, and R. H. Unger, "Adipogenic capacity and the susceptibility to type 2 diabetes and metabolic syndrome," *Proceedings of the National Academy of Sciences of the United States of America*, vol. 105, no. 16, pp. 6139–6144, 2008.
- [46] K. J. Strissel, Z. Stancheva, H. Miyoshi et al., "Adipocyte death, adipose tissue remodeling, and obesity complications," *Diabetes*, vol. 56, no. 12, pp. 2910–2918, 2007.
- [47] C. Duval, U. Thissen, S. Keshtkar et al., "Adipose tissue dysfunction signals progression of hepatic steatosis towards nonalcoholic steatohepatitis in C57Bl/6 mice," *Diabetes*, vol. 59, no. 12, pp. 3181–3191, 2010.
- [48] L. Shi, R. Kishore, M. R. McMullen, and L. E. Nagy, "Lipopolysaccharide stimulation of ERK1/2 increases TNF- α production via Egr-1," *American Journal of Physiology—Cell Physiology*, vol. 282, no. 6, pp. C1205–C1211, 2002.
- [49] M. Poggi, D. Bastelica, P. Gual et al., "C3H/HeJ mice carrying a toll-like receptor 4 mutation are protected against the development of insulin resistance in white adipose tissue in response to a high-fat diet," *Diabetologia*, vol. 50, no. 6, pp. 1267–1276, 2007.
- [50] D. M. Tsukumo, M. A. Carvalho-Filho, J. B. Carnevali et al., "Loss-of-function mutation in toll-like receptor 4 prevents diet-induced obesity and insulin resistance," *Diabetes*, vol. 56, no. 8, pp. 1986–1998, 2007.
- [51] J. Y. Lee, K. H. Sohn, S. H. Rhee, and D. Hwang, "Saturated fatty acids, but not unsaturated fatty acids, induce the expression of cyclooxygenase-2 mediated through toll-like receptor 4," *Journal of Biological Chemistry*, vol. 276, no. 20, pp. 16683–16689, 2001.
- [52] M. Itoh, T. Suganami, N. Satoh et al., "Increased adiponectin secretion by highly purified eicosapentaenoic acid in rodent models of obesity and human obese subjects," *Arteriosclerosis, Thrombosis, and Vascular Biology*, vol. 27, no. 9, pp. 1918–1925, 2007.
- [53] A. Kosteli, E. Sugaru, G. Haemmerle et al., "Weight loss and lipolysis promote a dynamic immune response in murine

- adipose tissue,” *Journal of Clinical Investigation*, vol. 120, no. 10, pp. 3466–3479, 2010.
- [54] M. Ichioka, T. Suganami, N. Tsuda et al., “Increased expression of macrophage-inducible C-type lectin in adipose tissue of obese mice and humans,” *Diabetes*, vol. 60, no. 3, pp. 819–826, 2011.
- [55] S. Yamasaki, E. Ishikawa, M. Sakuma, H. Hara, K. Ogata, and T. Saito, “Mincle is an ITAM-coupled activating receptor that senses damaged cells,” *Nature Immunology*, vol. 9, no. 10, pp. 1179–1188, 2008.
- [56] S. Cinti, G. Mitchell, G. Barbatelli et al., “Adipocyte death defines macrophage localization and function in adipose tissue of obese mice and humans,” *Journal of Lipid Research*, vol. 46, no. 11, pp. 2347–2355, 2005.
- [57] C. R. Stewart, L. M. Stuart, K. Wilkinson et al., “CD36 ligands promote sterile inflammation through assembly of a toll-like receptor 4 and 6 heterodimer,” *Nature Immunology*, vol. 11, no. 2, pp. 155–161, 2010.
- [58] T. A. Seimon, M. J. Nadolski, X. Liao et al., “Atherogenic lipids and lipoproteins trigger CD36-TLR2-dependent apoptosis in macrophages undergoing endoplasmic reticulum stress,” *Cell Metabolism*, vol. 12, no. 5, pp. 467–482, 2010.
- [59] F. T. Schulthess, F. Paroni, N. S. Sauter et al., “CXCL10 impairs β cell function and viability in diabetes through TLR4 signaling,” *Cell Metabolism*, vol. 9, no. 2, pp. 125–139, 2009.
- [60] K. Schroder and J. Tschopp, “The Inflammasomes,” *Cell*, vol. 140, no. 6, pp. 821–832, 2010.
- [61] K. L. Rock, E. Latz, F. Ontiveros, and H. Kono, “The sterile inflammatory response,” *Annual Review of Immunology*, vol. 28, pp. 321–342, 2010.
- [62] R. Zhou, A. Tardivel, B. Thorens, I. Choi, and J. Tschopp, “Thioredoxin-interacting protein links oxidative stress to inflammasome activation,” *Nature Immunology*, vol. 11, no. 2, pp. 136–140, 2010.
- [63] R. Stienstra, L. A. Joosten, T. Koenen et al., “The inflammasome-mediated caspase-1 activation controls adipocyte differentiation and insulin sensitivity,” *Cell Metabolism*, vol. 12, no. 6, pp. 593–605, 2010.
- [64] B. Vandanmagsar, Y.-H. Youm, A. Ravussin et al., “The NLRP3 inflammasome instigates obesity-induced inflammation and insulin resistance,” *Nature Medicine*, vol. 17, no. 2, pp. 179–189, 2011.
- [65] S. L. Masters, A. Dunne, and S. L. Subramanian, “Activation of the NLRP3 inflammasome by islet amyloid polypeptide provides a mechanism for enhanced IL-1 β in type 2 diabetes,” *Nature Immunology*, vol. 11, no. 10, pp. 897–904, 2010.
- [66] P. Duewell, H. Kono, K. J. Rayner et al., “NLRP3 inflammasomes are required for atherogenesis and activated by cholesterol crystals,” *Nature*, vol. 464, no. 7293, pp. 1357–1361, 2010.

Increased Expression of Macrophage-Inducible C-type Lectin in Adipose Tissue of Obese Mice and Humans

Masayuki Ichioka,¹ Takayoshi Suganami,¹ Naoto Tsuda,¹ Ibuki Shirakawa,¹ Yoichiro Hirata,² Noriko Satoh-Asahara,³ Yuri Shimoda,¹ Miyako Tanaka,¹ Misa Kim-Saijo,¹ Yoshihiro Miyamoto,⁴ Yasutomi Kamei,¹ Masataka Sata,² and Yoshihiro Ogawa^{1,5}

OBJECTIVE—We have provided evidence that saturated fatty acids, which are released from adipocytes via macrophage-induced adipocyte lipolysis, serve as a naturally occurring ligand for the Toll-like receptor (TLR) 4 complex in macrophages, thereby aggravating obesity-induced adipose tissue inflammation. The aim of this study was to identify the molecule(s) activated in adipose tissue macrophages in obesity.

RESEARCH DESIGN AND METHODS—We performed a cDNA microarray analysis of coculture of 3T3-L1 adipocytes and RAW264 macrophages. Cultured adipocytes and macrophages and the adipose tissue of obese mice and humans were used to examine mRNA and protein expression.

RESULTS—We found that macrophage-inducible C-type lectin (Mincle; also called Clec4e and Clec5f9), a type II transmembrane C-type lectin, is induced selectively in macrophages during the interaction between adipocytes and macrophages. Treatment with palmitate, a major saturated fatty acid released from 3T3-L1 adipocytes, induced Mincle mRNA expression in macrophages at least partly through the TLR4/nuclear factor (NF)- κ B pathway. Mincle mRNA expression was increased in parallel with macrophage markers in the adipose tissue of obese mice and humans. The obesity-induced increase in Mincle mRNA expression was markedly attenuated in C3H/HeJ mice with defective TLR4 signaling relative to control C3H/HeN mice. Notably, Mincle mRNA was expressed in bone-marrow cell (BMC)-derived proinflammatory M1 macrophages rather than in BMC-derived anti-inflammatory M2 macrophages in vitro.

CONCLUSIONS—Our data suggest that Mincle is induced in adipose tissue macrophages in obesity at least partly through the saturated fatty acid/TLR4/NF- κ B pathway, thereby suggesting its pathophysiologic role in obesity-induced adipose tissue inflammation. *Diabetes* 60:819–826, 2011

Adipose tissue of obese animals and humans is characterized by adipocyte hypertrophy, followed by increases in angiogenesis, macrophage infiltration, and extracellular matrix and unbalanced production of pro- and anti-inflammatory adipocytokines (1–3). The dynamic change seen in adipose tissue during the course of obesity has been referred to as adipose tissue remodeling (4). Given their multifunctional roles in a variety of biological contexts, macrophages should play a central role in adipose tissue remodeling, thereby regulating adipocytokine production (2,4). Recent studies have pointed to at least two different polarization states of adipose tissue macrophages: M1 or “classically activated” (or proinflammatory) macrophages (5), which are induced by proinflammatory mediators such as lipopolysaccharide (LPS) and Th1 cytokine interferon (IFN)- γ , and M2 or “alternatively activated” (or anti-inflammatory) macrophages, which are generated in vitro by exposure to Th2 cytokines such as interleukin (IL)-4 and IL-13. It is noteworthy that macrophages, which are infiltrated into the adipose tissue during the course of obesity, exhibit the phenotypic switch from M2 to M1 polarization (6).

To explore the molecular mechanism underlying the crosstalk between adipocytes and macrophages during the course of adipose tissue remodeling, we have developed an in vitro coculture system composed of 3T3-L1 adipocytes and RAW264 macrophages and provided evidence that a paracrine loop involving saturated fatty acids and tumor necrosis factor (TNF)- α derived from adipocytes and macrophages, respectively, establishes a vicious cycle, thereby accelerating the inflammatory change in the adipose tissue in obesity (7). Interestingly, saturated fatty acids, which are released via macrophage-induced adipocyte lipolysis, may act as naturally occurring ligands for the Toll-like receptor (TLR) 4 complex, which is essential for the recognition of LPS, to induce nuclear factor (NF)- κ B activation in macrophages (8). With the aid of the coculture system, we recently have identified activating transcription factor 3, a member of basic leucine zipper-type transcription factors, which is induced in adipose tissue macrophages through the saturated fatty acid/TLR4 pathway, thereby regulating transcriptionally the obesity-induced macrophage activation (9). We, therefore, think the coculture system would provide a unique in vitro experimental system with which to investigate the molecular basis underlying obesity-induced adipose tissue inflammation.

Through a combination of cDNA microarray analyses of the coculture of 3T3-L1 adipocytes and RAW264 macrophages (7), we found that macrophage-inducible C-type

From the ¹Department of Molecular Medicine and Metabolism, Tokyo Medical and Dental University, Tokyo, Japan; the ²Department of Cardiovascular Medicine, Institute of Health Biosciences, The University of Tokushima Graduate School, Tokushima, Japan; the ³Division of Diabetic Research, Clinical Research Institute, Kyoto Medical Center, Kyoto, Japan; the ⁴Department of Medicine, Division of Atherosclerosis and Diabetes, National Cardiovascular Center Hospital, Osaka, Japan; and the ⁵Global Center of Excellence Program, International Research Center for Molecular Science in Tooth and Bone Diseases, Medical Research Institute, Tokyo Medical and Dental University, Tokyo, Japan.

Corresponding author: Yoshihiro Ogawa, ogawa.mmm@mri.tmd.ac.jp, or Takayoshi Suganami, suganami.mmm@mri.tmd.ac.jp.

Received 21 June 2010 and accepted 27 December 2010.

DOI: 10.2337/db10-0864

This article contains Supplementary Data online at <http://diabetes.diabetesjournals.org/lookup/suppl/doi:10.2337/db10-0864/-DC1>.

© 2011 by the American Diabetes Association. Readers may use this article as long as the work is properly cited, the use is educational and not for profit, and the work is not altered. See <http://creativecommons.org/licenses/by-nc-nd/3.0/> for details.

lectin (*Mincle*; also called *Clec4e* and *Clecsf9*), a type II transmembrane C-type lectin, is induced selectively in macrophages during the interaction between adipocytes and macrophages. *Mincle* originally was identified as a transcriptional target of CCAAT/enhancer binding protein β in macrophages in response to proinflammatory stimuli such as LPS, TNF- α , IL-6, and IFN- γ (10). Our data also suggest that *Mincle* is induced in M1 macrophages in the adipose tissue in obesity through the saturated fatty acid/TLR4/NF- κ B pathway. This study is the first detailed analysis of a C-type lectin in adipose tissue macrophages, thereby providing a novel insight into the molecular mechanism underlying adipose tissue inflammation.

RESEARCH DESIGN AND METHODS

Reagents. LPS (from *Escherichia coli* O111: B4) and BAY11-7085, an NF- κ B inhibitor, were purchased from Sigma (San Diego, CA) and Merck (Whitehouse Station, NJ), respectively. Palmitate and oleate were purchased from Sigma, solubilized in ethanol, and conjugated with fatty acid- and immunoglobulin-free BSA (Sigma) at a molar ratio of 10 to 1 (fatty acids to BSA) in a low-serum medium as described (7). The concentrations of palmitate and oleate used in this study (<200 μ mol/L) were within the physiologic range. All other reagents were purchased from Sigma or Nacalai Tesque (Kyoto, Japan), unless otherwise described.

Animals. Male C3H/HeJ (HeJ) mice, which have defective LPS signaling attributed to a missense mutation in the *TLR4* gene (11), and control C3H/HeN (HeN) mice were purchased from CLEA Japan (Tokyo, Japan). Male C57BL/6 J leptin-deficient *ob/ob* mice and their wild-type littermates were purchased from Charles River Japan (Tsukuba, Japan). The animals were housed in individual cages in a temperature-, humidity-, and light-controlled room (12-h light and 12-h dark cycle) and were allowed free access to water and standard diet (Oriental MF; 362 kcal/100 g, 5.4% energy as fat; Oriental Yeast, Tokyo, Japan), unless otherwise noted. In some experiments, mice were given free access to water and either the standard diet (SD) or the high-fat diet (HFD) (D12492; 556 kcal/100 g, 60% energy as fat; Research Diets, New Brunswick, NJ) for 16 weeks. All animal experiments were conducted according to the guidelines of the Tokyo Medical and Dental University Committee on Animal Research (no. 100098).

Cell culture. The RAW264 macrophage cell line (Riken BioResource Center, Tsukuba, Japan) and 3T3-L1 preadipocytes (American Type Culture Collection, Manassas, VA) were maintained in Dulbecco's modified Eagle's medium (Nacalai Tesque) containing 10% FBS (7,8). Generation of RAW264 macrophages overexpressing a superrepressor form of the inhibitor of κ B ($\text{I}\kappa\text{B}\alpha$) (SR- $\text{I}\kappa\text{B}\alpha$; a degradation-resistant mutant of $\text{I}\kappa\text{B}\alpha$) were reported previously (9,12,13). Peritoneal and bone-marrow-derived macrophages were prepared as described (8,14,15). For macrophage polarization experiments, bone-marrow cell (BMC)-derived macrophages were cultured for 24 h in Iscove's modified Dulbecco's medium (Invitrogen, Carlsbad, CA) containing 5% FBS supplemented with 10 ng/mL LPS and 20 ng/mL IFN- γ (for M1 polarization) or 10 ng/mL IL-4 (for M2 polarization) (5). Control macrophages were prepared in Iscove's modified Dulbecco's medium containing 5% FBS alone.

Coculture of adipocytes and macrophages. Coculture of 3T3-L1 adipocytes and macrophages (RAW264 or peritoneal macrophages) in the contact system was performed as described (7,8). In brief, serum-starved differentiated 3T3-L1 adipocytes ($\sim 0.5 \times 10^6$ cells) were cultured in a 35-mm dish, and macrophages (1.0×10^5 cells) were plated onto 3T3-L1 adipocytes (contact coculture) (Fig. 1A). The cells were cultured with direct cell-to-cell contact and harvested after a 24-h incubation, unless otherwise described. As a control (control culture), adipocytes and macrophages, the numbers of which were equal to those in the coculture, were cultured separately and mixed after harvest. Our previous data suggest that there is no apparent difference in macrophage cell number between the coculture and control culture (7).

In some experiments, we cocultured RAW264 macrophages with adipose tissue explants in the transwell system, in which adipose tissue explants of 8-week-old C57BL/6 J mice were plated in a transwell insert with a 0.4- μ m porous membrane (Corning, Corning, NY) to separate them from RAW264 macrophages (Supplementary Fig. 1A). After incubation for 8 h, RAW264 macrophages in the lower well were harvested.

cDNA microarray analysis. cDNA microarray analysis was performed using mouse genome 430A 2.0 (Affymetrix, Santa Clara, CA) as described (8,9). Total RNA was prepared from the contact coculture of 3T3-L1 adipocytes and RAW264 macrophages, the control culture, and 3T3-L1 adipocytes alone (Fig. 1A). In this experiment, we cocultured the cells for 8 h. We also performed

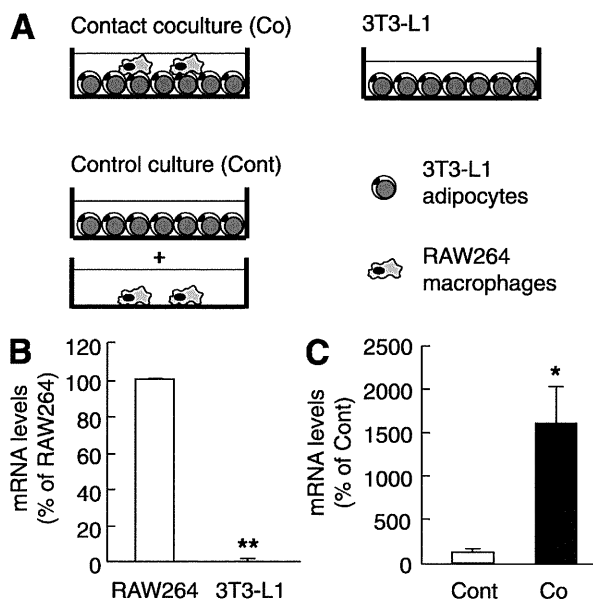


FIG. 1. Identification of *Mincle* as a target gene upregulated in the coculture of 3T3-L1 adipocytes and RAW264 macrophages. **A:** Illustration of the contact coculture system composed of 3T3-L1 adipocytes and RAW264 macrophages. **B:** *Mincle* mRNA expression in RAW264 and 3T3-L1. **C:** Effect of coculture on *Mincle* mRNA expression. $n = 4$. * $P < 0.05$; ** $P < 0.01$.

a hierarchical clustering analysis using GeneSpring (Agilent Technologies, Palo Alto, CA).

Quantitative real-time PCR. Total RNA was extracted from various tissues and cultured cells using a TRIzol reagent (Invitrogen), and quantitative real-time PCR was performed with an ABI Prism 7000 Sequence Detection System using PCR Master Mix reagent (Applied Biosystems, Foster City, CA) as described (7–9). Primers used to detect mouse and human mRNAs are described in Supplementary Tables 1 and 2, respectively. Levels of mRNA were normalized to those of 36B4 mRNA (for mouse) or β -actin (for humans).

Preparation of rabbit polyclonal anti-mouse *Mincle* antibody and Western blot analysis. Details are shown in the Supplementary Research Design and Methods.

Human studies on *Mincle* expression in the adipose tissue and circulating monocytes. Details are shown in Supplementary Research Design and Methods and Supplementary Table 3. The study protocol was approved by the ethical committee on human research of The University of Tokushima Graduate School, Kyoto Medical Center, and the Tokyo Medical and Dental University.

Statistical analysis. Data were expressed as the means \pm SE. Statistical analysis was performed using ANOVA. $P < 0.05$ was considered to be statistically significant. In the human study, linear regression analysis was used to evaluate the relationship between *Mincle* mRNA levels and BMI.

RESULTS

Coculture-induced *Mincle* mRNA expression in macrophages. To screen the gene(s) that are upregulated selectively in macrophages during the interaction between adipocytes and macrophages, we performed cDNA microarray analysis of the coculture of 3T3-L1 adipocytes and RAW264 macrophages in the contact system (Fig. 1A). There were 316 genes upregulated (>1.5-fold) in the coculture of 3T3-L1 adipocytes and RAW264 macrophages relative to the control culture, including chemokines, proinflammatory cytokines, and acute-phase reactants (Supplementary Table 4). We also compared the control culture with 3T3-L1 adipocytes alone to examine macrophage selective expression (Supplementary Table 4). In this study, we have focused on *Mincle*, a type II transmembrane C-type

lectin in macrophages, for the following reasons. First, Mincle is induced by LPS (10). Second, Mincle is selectively expressed in macrophages (Supplementary Table 4). We confirmed by real-time PCR that Mincle exhibits highly selective expression in RAW264 macrophages relative to 3T3-L1 adipocytes and is markedly upregulated by the coculture ($P < 0.01$ and $P < 0.05$) (Fig. 1B and C, respectively). Last, Mincle acts as a pathogen sensor to induce proinflammatory cytokine and chemokine expression such as TNF- α and macrophage inflammatory protein 2 (16–19). Indeed, cluster analysis revealed that Mincle shows a similar expression pattern with eight genes (Supplementary Fig. 2), which are all related to inflammatory responses. These observations, taken together, suggest that Mincle is selectively induced in macrophages during the interaction between adipocytes and macrophages.

Role of the saturated fatty acid/TLR4/NF- κ B pathway in Mincle expression. Because saturated fatty acids are a major adipocyte-derived paracrine mediator of inflammation in macrophages (8,20), we examined the effect of palmitate, a major saturated fatty acid released from 3T3-L1 adipocytes, on Mincle mRNA expression in RAW264 or peritoneal macrophages. Treatment with palmitate for 24 h induced Mincle mRNA and protein expression in RAW264 macrophages in a dose-dependent manner (Fig. 2A–C). On the other hand, there was no apparent change in Mincle mRNA and protein expression when it was treated with unsaturated fatty acid oleate (Fig. 2A–C). We also found that palmitate, as well as LPS, induces Mincle mRNA expression in peritoneal macrophages of control C3H/HeN mice. Importantly, the induction was markedly inhibited in peritoneal macrophages of TLR4 signal-deficient C3H/HeJ mice ($P < 0.01$) (Fig. 2D). Moreover, treatment with BAY11-7085, an NF- κ B inhibitor, significantly inhibited the palmitate-induced Mincle mRNA expression in RAW264 macrophages ($P < 0.05$) (Fig. 2E). The palmitate-induced Mincle mRNA expression also was significantly reduced in RAW264 macrophages overexpressing SR-I κ B α , a dominant-negative form of I κ B α , relative to those without SR-I κ B α expression ($P < 0.01$) (Fig. 2F). These observations suggest that the TLR4/NF- κ B pathway is involved in the saturated fatty acid-induced Mincle expression in macrophages.

To elucidate the role of TLR4 in the coculture-induced Mincle mRNA expression, we performed the coculture of 3T3-L1 adipocytes and peritoneal macrophages of C3H/HeJ or C3H/HeN mice. Coculture of 3T3-L1 adipocytes with C3H/HeN peritoneal macrophages resulted in the marked upregulation of Mincle mRNA, which was significantly inhibited in the coculture with C3H/HeJ peritoneal macrophages ($P < 0.05$) (Fig. 2G). Moreover, treatment with BAY11-7085 effectively inhibited the coculture-induced Mincle mRNA expression ($P < 0.05$) (Fig. 2H). These observations, taken together, suggest the role of the TLR4/NF- κ B pathway in the coculture-induced Mincle mRNA expression.

Mincle expression in adipose tissue of obese mice. Because there is no previous report on the tissue distribution of Mincle expression in vivo, we next examined the tissue distribution of Mincle mRNA in genetically obese *ob/ob* mice and wild-type mice (Fig. 3A). Real-time PCR analysis revealed that Mincle mRNA is expressed most abundantly in the spleen of lean wild-type mice. Other organs such as the liver, colon, intestine, and adipose tissue also expressed Mincle mRNA, although to a lesser extent than in the spleen. Similar to macrophage marker F4/80 and M1 macrophage marker CD11c, Mincle mRNA expression

was markedly increased in the adipose tissue of *ob/ob* mice relative to wild-type mice. We also observed a significant upregulation of Mincle mRNA in the adipose tissue of diet-induced obese mice ($P < 0.01$) (Fig. 3B). Collagenase digestion of adipose tissue, which is validated by F4/80 and adiponectin mRNA expression (9), revealed that Mincle mRNA expression is predominantly detected in the stromal-vascular fraction, which was markedly increased in *ob/ob* mice relative to wild-type mice ($P < 0.05$) (Fig. 3C). In this study, there was a significant increase in Mincle mRNA expression in the heart and liver ($P < 0.01$ and $P < 0.05$, respectively) (Fig. 3A). These observations, taken together, suggest that Mincle is markedly upregulated mostly in adipose tissue macrophages in obesity.

Role of TLR4 in obesity-induced Mincle mRNA expression in vivo. Using C3H/HeJ and C3H/HeN mice fed an HFD or an SD for 16 weeks, we examined the involvement of TLR4 signaling in obesity-induced Mincle mRNA expression in vivo. We previously demonstrated that the weight gain of C3H/HeJ mice as a result HFD feeding is roughly comparable with that of C3H/HeN mice (9,21). We also found that there is no appreciable difference in the number of F4/80-positive macrophages between the genotypes (9,21). In this study, Mincle mRNA expression in adipose tissue on an HFD was significantly attenuated in C3H/HeJ mice relative to C3H/HeN mice ($P < 0.05$), whereas there was no appreciable difference between the genotypes on an SD (Fig. 4A). Similarly, mRNA expression of the M1 macrophage marker, CD11c, tended to be decreased in the adipose tissue of C3H/HeJ mice relative to C3H/HeN mice, although CD11c mRNA expression was significantly increased on an HFD relative to an SD in both genotypes (Fig. 4B). These observations suggest that TLR4 signaling plays an important role in the obesity-induced Mincle mRNA expression in adipose tissue macrophages in vivo.

Mincle mRNA expression in BMC-derived M1 macrophages in vitro. To further explore Mincle mRNA expression in M1 versus M2 macrophages, we examined Mincle mRNA expression in BMC-derived M1 and M2 macrophages in vitro. We confirmed that TNF- α and inducible nitric oxide (NO) synthase mRNAs are expressed exclusively in BMC-derived M1 macrophages (Fig. 5A), whereas BMC-derived M2 macrophages show substantial expression of arginase 1 and mannose receptor mRNAs (Fig. 5B). In this study, Mincle mRNA was predominantly expressed in BMC-derived M1 macrophages (Fig. 5C). In contrast, no appreciable amount of Mincle mRNA was detected in BMC-derived M2 macrophages (Fig. 5C). These observations suggest that Mincle is expressed in M1 macrophages rather than in M2 macrophages in vitro.

Mincle mRNA expression in the adipose tissue and circulating monocytes of obese subjects. We also examined Mincle mRNA expression in human subcutaneous adipose tissue. We did not observe significant differences in blood pressure and serum triglycerides, HDL cholesterol, LDL cholesterol, and HbA_{1c} levels between the groups (Table 1). On the other hand, there was a tendency of increased expression of CD11c and CD68 mRNAs in the adipose tissue of obese subjects relative to nonobese subjects (Fig. 6A). In this study, Mincle mRNA expression was markedly increased in the adipose tissue of obese subjects relative to nonobese subjects ($P < 0.01$) (Fig. 6A). Linear regression analysis also revealed a significantly positive correlation between Mincle mRNA levels and BMI ($r^2 = 0.3589$, $P < 0.01$) (Fig. 6B).

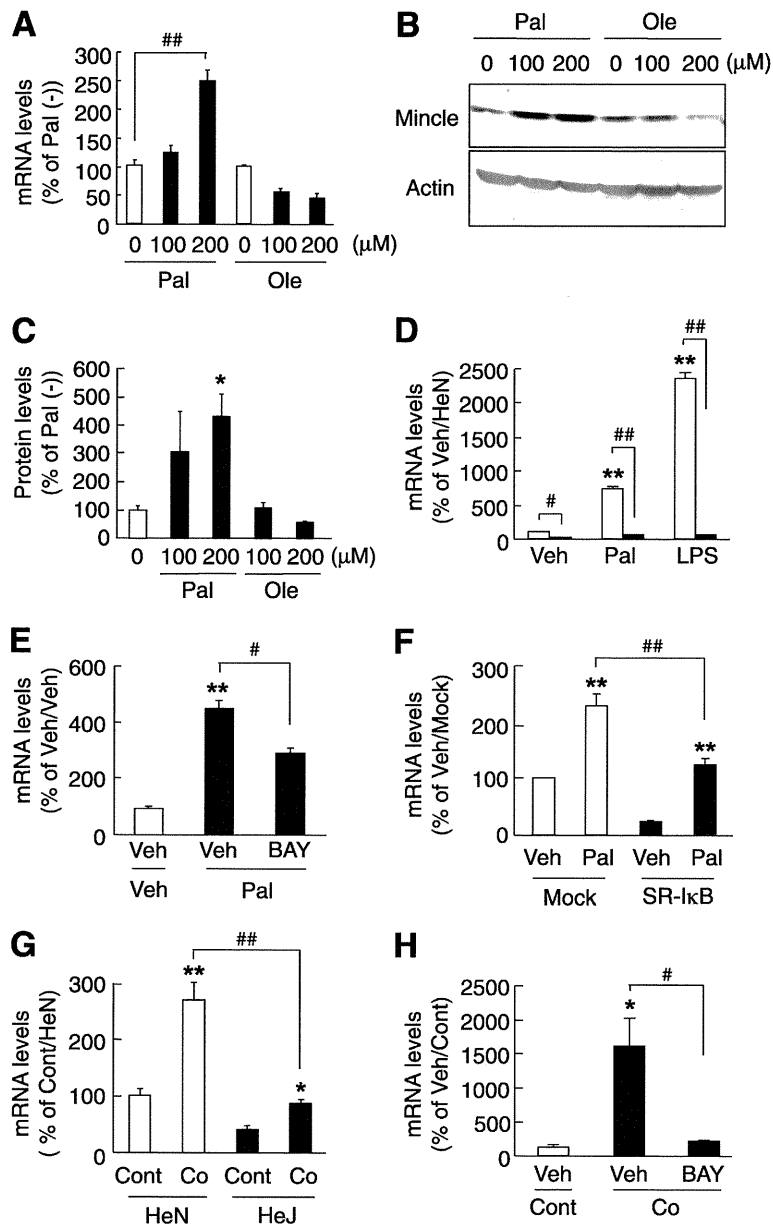


FIG. 2. Effect of palmitate on Mincle expression in cultured macrophages. *A–C:* Effect of palmitate (Pal) and oleate (Ole) on Mincle mRNA (*A*) and protein (*B* and *C*) expression in RAW264 macrophages. Representative Western blots (*B*) and quantitative relative protein expression (*C*) of Mincle. *D:* Mincle mRNA expression stimulated by palmitate (200 μ mol/L) and LPS (10 ng/mL) in peritoneal macrophages prepared from TLR4 signal-deficient C3H/HeJ (■, HeJ) and control C3H/HeN (□, HeN) mice. *E:* Effect of BAY11-7085 (BAY; an NF- κ B inhibitor) on the palmitate-induced Mincle mRNA expression in RAW264 macrophages. *F:* Effect of palmitate on Mincle mRNA expression in SR-I κ B α - (a dominant-negative form of I κ B α) and mock-overexpressing RAW264 (SR-I κ B and Mock, respectively) macrophages. *G:* Effect of coculture of 3T3-L1 adipocytes and peritoneal macrophages of C3H/HeJ and C3H/HeN mice on Mincle mRNA expression. *H:* Effect of BAY (1 μ mol/L) on coculture-induced Mincle mRNA expression. Co, coculture; Cont, control culture; Veh, vehicle. $n = 3–4$. * $P < 0.05$; ** $P < 0.01$ vs. each control; # $P < 0.05$; ## $P < 0.01$.

We further examined Mincle mRNA expression in circulating monocytes of nondiabetic subjects. We did not observe significant differences in diastolic blood pressure and serum lipid levels between the groups, whereas systolic blood pressure was significantly high in obese subjects relative to nonobese subjects ($P < 0.05$) (Supplementary Table 3). In this study, Mincle mRNA expression was significantly increased in the circulating monocytes of obese subjects relative to nonobese subjects ($P < 0.05$) (Fig. 7). In this setting, circulating monocytes of obese

subjects exhibited higher TNF- α and IL-6 mRNA expression and lower IL-10 mRNA expression than those of nonobese subjects (Fig. 7). Collectively, these observations suggest that Mincle expression is increased in the adipose tissue and circulating monocytes in obese subjects.

DISCUSSION

During the course of adipose tissue remodeling in obesity, infiltrating macrophages may participate in the inflammatory pathways that are activated in the adipose tissue (1,2,7).